

Article

Biological Activity of Newly Synthesized Benzimidazole and Benzothiazole 2,5-Disubstituted Furane Derivatives

Livio Racané ^{1,†}, Ivo Zlatar ^{2,†}, Nataša Perin ³, Maja Cindrić ³, Vedrana Radovanović ², Mihailo Banjanac ², Suresh Shanmugam ⁴, Marijana Radić Stojković ⁴, Karmen Brajša ^{2,*} and Marijana Hranjec ^{3,*}

¹ Department of Applied Chemistry, Faculty of Textile Technology, University of Zagreb, Prilaz baruna Filipovića 28a, 10000 Zagreb, Croatia; lracane@ttf.hr

² Pharmacology In Vitro, Fidelta Ltd., Prilaz baruna Filipovića 29, 10000 Zagreb, Croatia; ivo.zlatar@fidelta.eu (I.Z.); vedrana.radovanovic@fidelta.eu (V.R.); mihailo.banjanac@fidelta.eu (M.B.)

³ Department of Organic Chemistry, Faculty of Chemical Engineering and Technology, University of Zagreb, Marulićev trg 19, 10000 Zagreb, Croatia; nperin@fkit.hr (N.P.); mcindric@fkit.hr (M.C.)

⁴ Division of Organic Chemistry and Biochemistry, Ruđer Bošković Institute, Bijenička cesta 54, 10000 Zagreb, Croatia; suresh.shanmugam@irb.hr (S.S.); mradic@irb.hr (M.R.S.)

* Correspondence: karmen.brajsa@fidelta.eu (K.B.); mhranjec@fkit.hr (M.H.); Tel.: +385-1-4597245 (M.H.)

† These authors contributed equally.

Abstract: Newly designed and synthesized cyano, amidino and acrylonitrile 2,5-disubstituted furane derivatives with either benzimidazole/benzothiazole nuclei have been evaluated for antitumor and antimicrobial activity. For potential antitumor activity, the compounds were tested in 2D and 3D cell culture methods on three human lung cancer cell lines, A549, HCC827 and NCI-H358, with MTS cytotoxicity and BrdU proliferation assays in vitro. Compounds **5**, **6**, **8**, **9** and **15** have been proven to be compounds with potential antitumor activity with high potential to stop the proliferation of cells. In general, benzothiazole derivatives were more active in comparison to benzimidazole derivatives. Antimicrobial activity was evaluated with Broth microdilution testing (according to CLSI (Clinical Laboratory Standards Institute) guidelines) on Gram-negative *Escherichia coli* and Gram-positive *Staphylococcus aureus*. Additionally, *Saccharomyces cerevisiae* was included in testing as a eukaryotic model organism. Compounds **5**, **6**, **8**, **9** and **15** showed the most promising antibacterial activity. In general, the compounds showed antitumor activity, higher in 2D assays in comparison with 3D assays, on all three cell lines in both assays. In natural conditions, compounds with such an activity profile (less toxic but still effective against tumor growth) could be promising new antitumor drugs. Some of the tested compounds showed antimicrobial activity. In contrast to ctDNA, the presence of nitro group or chlorine in selected furane-benzothiazole structures did not influence the binding mode with AT-DNA. All compounds dominantly bound inside the minor groove of AT-DNA either in form of monomers or dimer and higher-order aggregates.

Keywords: amidines; acrylonitriles; benzimidazoles; benzothiazoles; furanes; antitumor activity; DNA binding



Citation: Racané, L.; Zlatar, I.; Perin, N.; Cindrić, M.; Radovanović, V.; Banjanac, M.; Shanmugam, S.; Stojković, M.R.; Brajša, K.; Hranjec, M. Biological Activity of Newly Synthesized Benzimidazole and Benzothiazole 2,5-Disubstituted Furane Derivatives. *Molecules* **2021**, *26*, 4935. <https://doi.org/10.3390/molecules26164935>

Academic Editor: René Csuk

Received: 14 July 2021

Accepted: 11 August 2021

Published: 14 August 2021

Publisher's Note: MDPI stays neutral with regard to jurisdictional claims in published maps and institutional affiliations.



Copyright: © 2021 by the authors. Licensee MDPI, Basel, Switzerland. This article is an open access article distributed under the terms and conditions of the Creative Commons Attribution (CC BY) license (<https://creativecommons.org/licenses/by/4.0/>).

1. Introduction

Among all known nitrogen heterocycles, benzimidazole and benzothiazole moieties have been recognized as important and well-known constituents of biologically important molecules in medicinal and pharmaceutical chemistry [1–5]. Due to their wide range of biological activities, these heterocycles are still unavoidable structural motifs in the rational design of novel drugs.

Among their versatile pharmacological features, the most important ones are antimicrobial, antitumor, antiviral, anti-inflammatory, antihistaminic, antioxidant, etc. [5–8]. One of the most commonly used classes of chemotherapeutic agents in medicinal chemistry are still molecules that interact with DNA/RNA [9–12].

Since amidines are also important structural parts of numerous biologically active compounds, such as many important medical and biochemical agents, suchlike derivatives contribute significantly to the molecule/possible biological target complex stability through H-bonding and electrostatic interactions [13,14]. In several previously published papers we have proven that by incorporation of one or two positively charged amidine moieties at the end of the heteroaromatic benzimidazole/benzothiazole derivatives, we could significantly improve the biological activity [13–19]. Additionally, the amidine groups allowed and oriented the function of the heteroaromatic derivative toward the binding to an electronegatively charged molecule such as DNA/RNA. For example, we have shown that some benzimidazole and benzothiazole derivatives bearing amidine moiety showed strong antitumor activity by intercalating into ds-RNA and ct-DNA, or by binding into the minor groove of AT-DNA, ss-RNA or showed sequence-selective binding in the A-T rich side of ct-DNA [20,21]. Furthermore, the antimicrobial properties of dicationic molecules with amidine moieties similar to pentamidine have been studied since the beginning of the 20th century, showing activities against a number of pathogens [22,23]. Several suchlike derivatives have been proven to bind to the minor groove of DNA at AT-rich sites [24,25], which was confirmed by different biophysical studies [26] and several crystal structures. Some extensive work has been undertaken in the chemistry of 2,5-disubstituted furane derivatives bearing either one or two amidine moieties. Thus, diamidine furamide I (Figure 1) showed a broad spectrum of antimicrobial activities [27] while some other similar derivatives have been extensively studied in phase I and/or II of clinical trials.

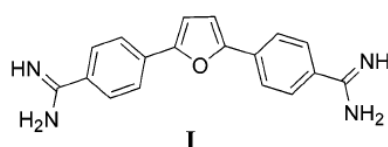


Figure 1. The structure of diamidine furamide analogue I.

The mode of biological action which include the binding to DNA and subsequent inhibition of DNA dependent enzymes has been proposed for these types of molecules [28]. Furthermore, some 2,5-bis(4-amidinophenyl)furan and their substituted amidino derivatives were shown to be effective in vivo at a submicromolar per kilogram body weight dosage against *P. carinii* in the immunosuppressed rat model [29,30]. A group of authors has studied the biological activity of aza-analogues of furamide by replacing the phenyl ring with pyridine, but none of the derivatives appeared to have significant advantages over the furan analogues [31].

Taking into account that both benzimidazoles and benzothiazoles are among the most privileged heterocyclic subunits and important building blocks in medicinal chemistry, and the important role of the amidino moiety at the end of the heteroaromatic molecules, we have synthesized novel 2,5-disubstituted cyano and amidino furane derivatives. Additionally, since the cyano group has a positive influence on biological activity and acrylonitriles bearing heteroaromatic or aromatic moieties have been recognized as promising biologically active compounds, we have designed and synthesized novel acrylonitrile 2,5-furane derivatives bearing either benzimidazole or benzothiazole nuclei.

All newly designed compounds were tested for screening in vitro on human lung cancer cells on two-dimensional and three-dimensional cell culture assays.

At a very early stage of the R&D process of new oncology drugs, tests used in the screening phase to identify active molecules with antitumor activity are traditionally performed on tumor cell cultures grown in two-dimensional (2D) conditions that do not provide the same conditions to cells for growth and development as is the case in a living organism. The limitations of such 2D tests are the unnatural shape of the cells (flat), different gene expression, cellular environment, metabolism and other parameters. Therefore, in the last ten years, in vitro cell-based assays have been developed, with more similar conditions to the natural conditions, namely three-dimensional (3D) cultured

cell lines, such as morphology, growth and differentiation, metabolic activity and gene expression in comparison with cell grown in 2D cultures [32].

In previous research, we obtained the discrepancy of growth inhibitory concentrations (IC₅₀) values of NCE to examine their potential antitumor activity parallel on two-dimensional (2D) and three-dimensional (3D) cell culture assays with different tumor cell lines [33,34]. Therefore, the presented study involves compound testing in 2D and 3D cell cultures on three lung cell lines (A549, HCC827, NCI-H358) in parallel. As a 3D assay model, we used a “hanging-drop” model because the model allows avoidance of NCE interactions with other substrates used as carrier material, and compounds were tested on MTS assay due to determinate antitumor activity and BrdU assay for measurement of their antiproliferative activity. Both tests were performed in parallel in 2D and 3D grown cell cultures and IC₅₀ values were compared. As standard compounds, we used three chemotherapeutics (doxorubicin, vandetanib and staurosporine). All compounds were also tested for their antibacterial activity on *E. coli* and *S. aureus* as well as on *S. cerevisiae*.

As mentioned earlier, the study of non-covalent interactions of small molecules with DNA can help in the understanding of their mechanism of action and anticipation of the potential therapeutic significance of such interactions [35]. Estimation of the binding strength and binding mode of small molecule and DNA interactions was performed using UV/Vis, fluorescence and circular dichroism spectroscopy.

2. Results and Discussion

2.1. Chemistry

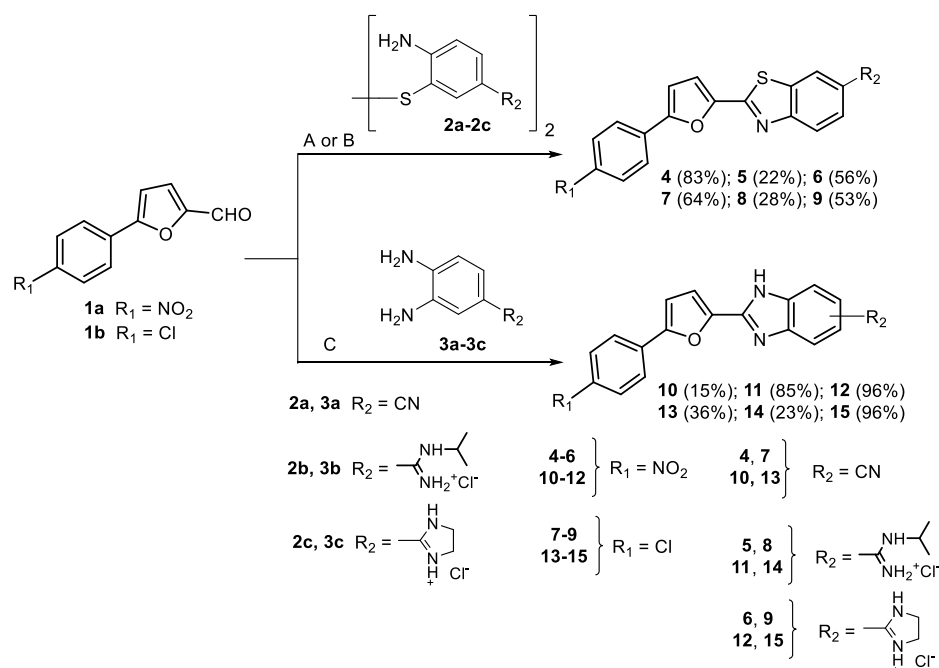
The cyano, amidino and acrylonitrile substituted 2,5-furane derivatives bearing benzimidazole or benzothiazole nuclei were synthesized according to the experimental procedures presented in Schemes 1 and 2. To ensure the efficient synthesis of targeted benzazole derivatives, our well-optimized methods for cyclocondensation to fused benzazole derivatives were used. Cyano and amidino substituted benzothiazole derivatives 4–9 were prepared following the recently developed green synthetic protocol from 2-aminophenyl disulfides and aromatic aldehydes by simple thermal reaction in glycerol, without the need for a catalyst [36]. Applying this condensation method, the corresponding furan-2-carbaldehydes 1a–1b and cyano-substituted 2-aminophenyldisulfide 2a [32] afforded nitrophenyl- and chlorophenyl- cyanobenzothiazole derivatives 4 and 7 in a very good yield. Condensation of the corresponding amidino-substituted 2-aminophenyldisulfides 2b–2c [37] with aldehydes 1a–1b afforded in a first step the crude free base of 6-(*N*-isopropyl-amidino)benzothiazole and 6-(2-imidazoliny)benzothiazole derivatives, which in a second step were converted by an excess of hydrochloric acid in 2-propanol in a targeted hydrochlorides 5–6 and 8–9 in moderate overall reaction yields. Cyano and amidino substituted benzimidazole derivatives 10–15 were prepared following the experimental protocol shown in Scheme 1.

Due to the reaction of cyclocondensation of 5-(4-nitro/chlorophenyl) substituted furan-2-carbaldehydes 1a–1b and 4-(cyano/*N*-isopropyl-amidino/4-(2-imidazoliny)-1,2-phenylene diamine hydrochlorides 2a–2c, corresponding 2,5-furyl-substituted benzimidazoles 10–15 were obtained in moderate reaction yields as a mixture of inseparable tautomers.

Amidino substituted 1,2-phenylenediamine 3b–3c were obtained in the acidic Pinner reaction from corresponding cyano substituted precursors according to the previously published procedures [13]. Acrylonitrile substituted 2,5-difurane derivatives bearing either benzimidazole 17–18 and 20–21 or benzothiazole 19 and 22 nuclei were synthesized according to the procedure shown in Scheme 2 in the reaction of condensation from 5-(4-nitro/chlorophenyl) substituted furan-2-carbaldehydes 1a–1b and 2-cyanomethylbenzimidazole/benzothiazole 16a–16c in absolute ethanol with piperidine as a base [38]. Derivatives 18 and 21 were obtained as a mixture of *E*- and *Z*-isomers.

The structures of all newly prepared cyano, amidino and acrylonitrile substituted benzimidazole/benzothiazole derivatives were confirmed by means of ¹H and ¹³C NMR spectroscopy as well as elemental analysis.

NMR analysis based on the values of chemical shifts and H-H coupling constants in the ^1H spectra confirmed the structures of the compounds. Furthermore, ^{13}C NMR chemical shifts additionally confirmed the suggested structures. Additionally, IR spectroscopy was used for the monitoring of the Pinner reaction due to the synthesis of benzimidazole precursors **3b–3c**.



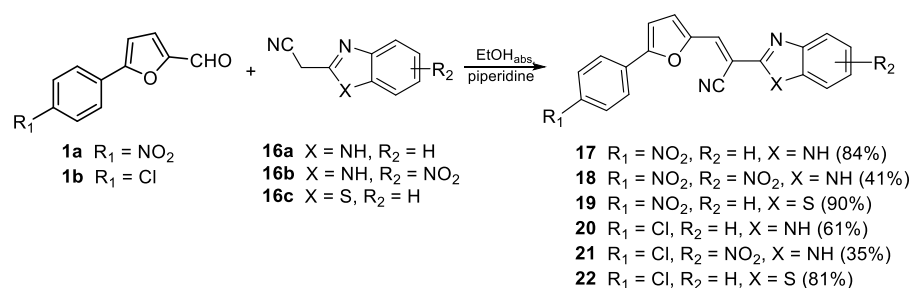
Reagents and conditions:

A; **2a**, glycerol, 165 °C, 45 min

B; i) **2b**, **2c** glycerol, 165 °C, 45 min, then NaOH pH 10-12; ii) 2-PROH/HCl, rt, 1-2h

C; **3a-c** EtOHaps/*p*-benzoquinone, reflux, 2.5-4 h

Scheme 1. Synthesis of cyano and amidino substituted derivatives **4–15**.



Scheme 2. Synthesis of acrylonitrile derivatives **17–22**.

2.2. Biology

2.2.1. Antiproliferative Activity and Cytotoxicity Assays in 2D and 3D Cell Culture Assays In Vitro

As cytotoxicity and proliferation assays readouts give two distinct characteristics of cells, we tested compounds in MTS cytotoxicity assay and BrdU proliferative assay. MTS assay gives us information about the number of living cells, in this case, metabolically active cells, whereas the BrdU proliferation assay gives a measure of the cell population in active division phase [39]. Both assays were performed in 2D and 3D assay formats. For the 2D cell assay format, we used classic two-dimensional in vitro assays [40] and as a 3D assay we used a hanging drop proliferation cell assay as previously described. We explored the activity of compounds on three human lung cancer cell lines, A549, HCC827 and NCI-H358. The compound activity was also tested on human lung fibroblast cell line MRC-5. A two-dimensional in vitro viability assay was performed on the MRC-5 cell line to see if tested

compounds are cytotoxic on normal cell lines in low concentrations. As standard drugs, we use doxorubicin, staurosporine and vandetanib, drugs with different modes of action. Doxorubicin interacts with DNA by intercalation and inhibits the synthesis of biomolecules, staurosporine is a protein kinase C (PKC) inhibitor and vandetanib multikinase inhibitor (VGFRs, EGFR and RET kinase) is an antitumor drug with potential use in a broad range of tumors types, especially thyroid and lung cancer. The results for each of the tested compounds are calculated as growth percentages from two independent concentrations curves compared with the untreated control cells after drug exposure and activity for each compound is presented as an IC₅₀ value calculated using the program GraphPadPrism software (La Jolla, CA, USA), v. 7.1.

The obtained IC₅₀ values of the tested compounds, as well as for the standard compounds in 2D and 3D cell culture systems in the cytotoxicity MTS assay for each of the three human lung cancer cell lines, are depicted in Table 1. As presented in Table 1, nitro substituted compound 5 bearing *iso*-propyl amidine moiety showed high antitumor activity in 2D assay on A549 and NCI-H358 cell lines and moderate on HCC827. Additionally, compound 5 has moderate cytotoxic activity on healthy MRC-5 lung fibroblasts, which is promising and can be a good start for further molecule optimization. Nitro substituted compound 6 with imidazoliny group showed high potential antitumor activity in 2D and 3D assay format against all three lung cancer cell cultures (A549 IC₅₀, 2.12 ± 0.21 μM and 4.01 ± 0.95 μM; HCC827 IC₅₀, 5.13 ± 0.97 μM and 7.02 ± 3.25 μM; NCI-H358 IC₅₀ for 0.85 ± 0.05 μM and 1.73 ± 0.01 μM). This compound also affected human lung fibroblast MRC-5 in 2D cytotoxicity assay (3.11 ± 0.26 μM). Compound 8, showed more prominent activity against A549 cancer cell line in both assay formats (A548 IC₅₀, 6.75 ± 0.19 μM and 9.31 ± 0.78 μM) in comparison to the other tested cell lines. Additionally, in 2D format on the other two cell lines, the activity of chloro substituted derivative 8 was significantly higher (HCC827 IC₅₀ 6.26 ± 0.33 μM; NCI-H358 IC₅₀ 6.48 ± 0.11 μM), in comparison with the activity in the 3D format assay (HCC827 IC₅₀ 20.46 ± 8.63 μM; NCI-H358 IC₅₀ 16.00 ± 9.38 μM). The same activity pattern was also shown by the imidazoliny substituted compounds 9 and 15 (high activity in 2D assay and medium activity in 3D assay).

Table 1. Cytotoxicity assays on tested compounds in 2D and 3D assays format.

Comp.	Cytotoxicity Assay IC ₅₀ Values (μM)							
	IC ₅₀ (μM) ± SD; n = 2							
	A549		HCC827		NCI-H358		MRC-5	
	2D	3D	2D	3D	2D	3D	2D	3D
4	>50	>100	>50	>100	>50	>100	>50	>100
5	8.76 ± 1.69	26.44 ± 13.37	19.33 ± 1.72	43.59 ± 6.45	9.97 ± 0.59	14.80 ± 0.57	21.65 ± 0.51	
6	2.12 ± 0.21	4.01 ± 0.95	5.13 ± 0.97	7.02 ± 3.25	0.85 ± 0.05	1.73 ± 0.01	3.11 ± 0.26	
7	>50	>100	>50	>100	>50	>100	>50	>100
8	6.74 ± 0.19	9.31 ± 0.78	6.26 ± 0.33	20.46 ± 8.63	6.48 ± 0.11	16.00 ± 9.38	9.88 ± 2.38	
9	4.39 ± 0.79	16.81 ± 2.61	5.9 ± 0.58	19.99 ± 7.92	4.48 ± 0.30	15.49 ± 0.07	6.65 ± 0.18	
10	>50	>100	>50	>100	>50	>100	>50	>100
11	>50	>100	>50	>100	>50	>100	>50	>100
12	>50	>100	>50	>100	>50	>100	>50	>100
13	>50	>100	>50	>100	>50	>100	>50	>100
14	>50	>100	>50	>100	31.07 ± 0.67	>100	>50	>100
15	24.29 ± 0.40	55.84 ± 8.29	22.70 ± 0.04	65.42 ± 5.04	19.39 ± 0.57	81.62 ± 7.71	>50	
17	>50	>100	>50	>100	>50	>100	>50	>100
18	>50	>100	>50	>100	3.50 ± 1.14	>100	>50	>100
19	>50	>100	>50	>100	>50	>100	>50	>100
20	>50	>100	43.53 ± 8.17	9.48 ± 1.15	31.08 ± 4.42	>100	>50	>100
21	>50	>100	>50	>100	3.58 ± 0.95	>100	>50	>100
22	>50	>100	>50	>100	>50	>100	>50	>100
Doxorubicin	1.31 ± 0.11	5.86 ± 1.10	0.32 ± 0.03	1.47 ± 0.12	0.15 ± 0.06	0.99 ± 0.15	0.60 ± 0.01	
Staurosporine	0.047 ± 0.007	0.095 ± 0.01	0.033 ± 0.002	0.002 ± 0.0001	0.041 ± 0.007	0.002 ± 0.001	0.031 ± 0.011	
Vandetanib	>25	>50	0.58 ± 0.03	0.16 ± 0.04	3.12 ± 35.99	0.38 ± 0.20	11.12 ± 0.00	

The reason that the compounds showed higher activity in 2D than in 3D assay format is expected to be due to how difficult it is for the compounds to penetrate 3D cell spheres and achieve full activity. Compound **20** was non-active on A549 and showed very low activity on other cell lines, except on HCC827 in 3D format assay ($9.48 \pm 1.15 \mu\text{M}$). Compounds, **8** and **9** showed similar activity on the MRC-5 normal lung fibroblast cell line, as could be seen on A549, HCC827 and NCI-H358 cancer cell lines, whereas compound **15** was non-active on MRC-5 cell line compared to three human lung cancer cell lines tested and the compound showed activity in A549, HCC827 and NCI-H358 cancer cell lines at the highest dose.

Active compounds are not selective for tested cancer cell lines, because the normal lung fibroblast cell line MRC-5 is also affected. This may have an impact on further compound development related to dose-limiting acute and chronic toxicities. Therefore, further optimization of the chemical structure of prepared compounds is required. Additionally, the IC_{50} values of control substances (doxorubicin, staurosporine and vandetanib) which showed the same non-selective activity against cancer test lines are presented also in the tables. Compound **15** showed very low activity on all cell lines and in both tested formats. All other tested compounds showed no activity in the cytotoxicity assay. If we compare the antiproliferation activity of the compounds presented in Table 2, we can conclude that all compounds, except compound **15**, active in viability assay, also showed antiproliferative activity but in slightly different ways. The most active compound **6** in viability assay also showed the most pronounced antiproliferative activity on all three tested cell lines, (A548 IC_{50} , $2.27 \pm 0.13 \mu\text{M}$ and $5.52 \pm 0.95 \mu\text{M}$; HCC827 (3D) IC_{50} $7.63 \pm 5.00 \mu\text{M}$; NCI-H358 IC_{50} for $1.10 \pm 0.001 \mu\text{M}$ and $2.36 \pm 1.17 \mu\text{M}$) except on HCC827 on 2 D format (IC_{50} $16.69 \pm 9.39 \mu\text{M}$) in which antiproliferative activity was moderate.

Table 2. Antiproliferation activity on 2,5-furane derivatives in 2D and 3D cell cultures.

Cpd.	Proliferation Assay IC_{50} Values (μM)					
	IC_{50} (μM) \pm SD; $n = 2$					
	A549		HCC827		NCI-H358	
	2D	3D	2D	3D	2D	3D
4	>50	>100	>50	>100	>50	>100
5	4.76 ± 1.03	65.93 ± 3.66	13.66 ± 3.13	14.69 ± 13.36	3.56 ± 0.18	14.29 ± 0.84
6	2.27 ± 0.13	5.52 ± 0.10	16.69 ± 9.39	7.63 ± 5.00	1.10 ± 0.001	2.36 ± 1.17
7	>50	>100	>50	>100	>50	>100
8	8.78 ± 3.62	19.94 ± 2.19	13.48 ± 0.81	17.75 ± 4.24	6.68 ± 0.15	11.27 ± 0.49
9	9.97 ± 5.37	17.01 ± 3.53	8.69 ± 2.79	20.28 ± 13.87	5.57 ± 0.81	6.39 ± 3.29
10	>50	>100	>50	>100	>50	>100
11	>50	>100	>50	>100	>50	>100
12	>50	>100	>50	16.85 ± 8.33	>50	>100
13	22.73 ± 0.54	>100	>50	>100	15.67 ± 0.86	>100
14	>50	>100	>50	>100	20.20 ± 0.71	>100
15	>50	>100	>50	>100	20.08 ± 2.82	>100
17	>50	>100	>50	>100	>50	>100
18	>50	>100	>50	>100	>50	>100
19	>50	>100	>50	>100	>50	>100
20	43.86 ± 54.27	>100	>50	0.16 ± 0.11	14.36 ± 6.46	>100
21	>50	>100	>50	>100	>50	>100
22	>50	>100	>50	>100	>50	>100
Doxorubicin	0.13 ± 0.01	0.48 ± 0.03	0.25 ± 0.28	1.89 ± 2.30	0.07 ± 0.04	2.30 ± 1.91
Staurosporine	0.035 ± 0.017	0.11 ± 0.001	0.004 ± 0.002	0.003 ± 0.002	0.0005 ± 0.00004	0.02 ± 0.01
Vandetanib	>25	>50	0.20 ± 0.11	0.08 ± 0.02	>25	0.38 ± 0.17

Compound **8** showed high activity against A549 and NCI-H358 cancer cell line in 2D assay formats (A549 IC_{50} , $8.78 \pm 3.62 \mu\text{M}$; NCI-H358 $6.68 \pm 15 \mu\text{M}$) but showed moderate activity in the 3D format assay (A548 IC_{50} , $19.94 \pm 2.19 \mu\text{M}$; NCI-H358 $11.27 \pm 0.49 \mu\text{M}$).

Additionally, antiproliferative activity was moderate for HCC827 for both assays formats (IC_{50} $13.48 \pm 0.81 \mu\text{M}$ and $17.75 \pm 4.24 \mu\text{M}$). Compounds **5** and **9** showed the same range and pattern of activity as in the viability assay (higher activity in 2D in comparison to 3D format assay) with the exception of NCI-H358 in 3D assay format, in which **9** showed a shift of activity from moderate activity in viability assay (IC_{50} $15.49 \pm 0.07 \mu\text{M}$) to high activity in the antiproliferative assay (IC_{50} $6.39 \pm 3.29 \mu\text{M}$). Compound **20** was again non-active on A549, showed moderate activity on other cell lines and high activity on HCC827 in the 3D format assay ($0.16 \pm 0.11 \mu\text{M}$) as in viability assay. Interestingly, besides **15**, which showed very low activity on all cell lines and in both tested formats in the viability test and was not active in the proliferative assay (except in NCI-H358, IC_{50} $20.08 \pm 2.82 \mu\text{M}$), compounds **13** and **14**, additionally showed low antiproliferative activity in the NCI-H358 cell line in 2D assay format (IC_{50} $15.67 \pm 0.86 \mu\text{M}$; IC_{50} $20.20 \pm 0.71 \mu\text{M}$). All other tested compounds showed no activity in the proliferative assay. The standard compounds showed the expected activity according to our previous experiments and the literature data. It is very difficult to compare IC_{50} values with the literature data, especially for 3D cultures, because the amount of such data is very limited and assay condition parameters are various.

In conclusion, 2,5-disubstituted benzothiazole derivatives **4–9** have more pronounced antiproliferative activity when compared to their benzimidazole analogues **10–15**. The most active compounds have proven to be both nitro **5** and chloro **8** substituted benzothiazole derivatives bearing *iso*-propyl amidine, as well as benzothiazoles **6** and **9** bearing the imidazolinylyl group. Furthermore, imidazolinylyl substituted benzothiazole derivatives **5–6** were more active in comparison to their *iso*-propyl amidine substituted analogues **8–9**. Additionally, the nitro group in comparison to chlorine substituents have improved antiproliferative activity. Regarding the 2,5-disubstituted benzimidazole derivatives **10–15**, the most active was cyano substituted derivative **13**, while nitro substituted derivative **12** bearing the imidazolinylyl group showed selective activity towards HCC827 cells. Among the acrylonitrile derivatives, the most pronounced activity was observed within the chloro substituted benzimidazole derivative **20**, with selective activity against HCC827 and NCI-H358 cells.

Therefore, it is always important to have standard compounds in every test run and observed quality control parameters of each growth curve. Due to the well-known fact that the 2,5-disubstituted furane derivatives are also potential antimicrobial agents, we tested the prepared derivatives on a primary antibacterial screening panel which includes *E. coli* ATCC 25,922 and *S. aureus* ATCC 29213. The summarized results are presented in Table 3. Only compound **15** showed significant antimicrobial activity against *S. aureus* (MIC $6.12 \mu\text{M}$) and moderate activity against *E. coli* (MIC $25 \mu\text{M}$). Both amidino substituted benzothiazole derivatives **8, 9** and *iso*-propyl amidino substituted benzimidazole **14** showed moderate activity to *S. aureus* (MIC 12.5, 25, $12.5 \mu\text{M}$). As we expected, the compounds that showed activity in MTS assay on eukaryotic cell lines were active against *S. cerevisiae* (**5, 6, 8, 9** and **15**).

Table 3. Antibacterial activity of prepared 2,5-disubstituted furanes.

Comp.	<i>E. coli</i> ATCC 25922	<i>S. aureus</i> ATCC 29213	<i>S. cerevisiae</i> ATCC 7752
	MIC (μM)		
4	>100	>100	>100
5	>100	50	12.5
6	>100	>100	1.6

Table 3. Cont.

Comp.	<i>E. coli</i> ATCC 25922	<i>S. aureus</i> ATCC 29213	<i>S. cerevisiae</i> ATCC 7752
	MIC (μM)		
7	>100	>100	>100
8	>100	12.5	6.25
9	>100	25	3.13
10	>100	>100	>100
11	>100	100	>100
12	>100	>100	100
13	>100	>100	>100
14	50	12.5	50
15	25	6.25	6.25
17	>100	>100	>100
18	>100	>100	>100
19	>100	>100	>100
20	>100	>100	>100
21	>100	>100	>100
22	>100	>100	>100
Ampicillin	4	2	>64
Ceftazidime	<0.125	16	>64
Ciprofloxacin	<0.125	0.25	>64
Gentamycin	0.5	0.25	>64
Voriconazole	>64	>64	<0.125

2.2.2. DNA Binding Study

Based upon the antiproliferative activity, compounds **5**, **6**, **8**, **9** and **15** were selected for the binding study with *calif thymus* DNA (ctDNA), which contains 58% AT and 42% GC nucleobases and represents a classical B-helix [41]. Polynucleotide addition to compound solutions resulted in an emission decrease in all selected compounds (Figure S5, Supporting information (SI)). The estimated binding constants K_s obtained by processing of fluorimetric titration data were of the same order of magnitude for all complexes of studied compounds with ctDNA ($\log K_s \approx 6$, Table S2, SI) [42].

The thermal stability of helices is usually affected by the non-covalent binding of small molecules to double-stranded nucleic acids [43]. We determined the ΔT_m value (the difference between the T_m value of free polynucleotide and a complex with a small molecule) for complexes of selected compounds with ctDNA and an alternating polynucleotide, poly(dAdT)₂. All studied compounds showed a greater stabilization effect of poly(dAdT)₂ compared to mixed base pair composition, ctDNA (Table 4). Because of this, we determined ΔT_m value with non-alternating AT-DNA, poly dA-poly dT as well.

Table 4. The ^a ΔT_m values ($^{\circ}\text{C}$) of studied ds- polynucleotides upon addition of ratio ^b $r = 0.3$ of **5**, **6**, **8**, **9**, and **15** at pH 7.0 (sodium cacodylate buffer, $I = 0.05 \text{ mol dm}^{-3}$).

^b $r = 0.3$	5	6	8	9	15
ctDNA	2.5	3.2	1.7	1.8	0.9
poly (dAdT) ₂	4.8	3.6	3.6	4.6	6.2
Poly dA-poly dT	5.5	5.6	4.3	15.2	11.7

^a Error in ΔT_m : $\pm 0.5 \text{ }^{\circ}\text{C}$; ^b $r = [\text{compound}]/[\text{polynucleotide}]$.

All compounds showed better stabilization effects with consecutive AT nucleobases, poly dA-poly dT than with poly(dAdT)₂ (Figure 2). Such preference toward AT basepairs is indicative of minor groove binders [44].

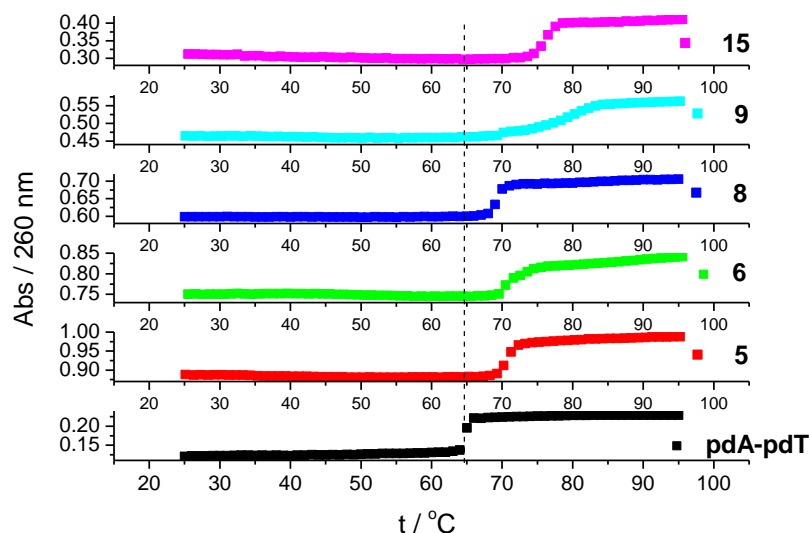


Figure 2. Melting curve of poly dA-poly dT upon addition of ratio, r ([compound]/[polynucleotide]) = 0.3 of 5, 6, 8, 9 and 15 at pH = 7.0 (buffer sodium cacodylate, $I = 0.05 \text{ mol dm}^{-3}$).

CD spectroscopy is often utilized for monitoring the specific signature of secondary structures of nucleic acids and structural changes resulting from interactions with various ligands or changes in conditions such as ionic strength, pH and temperature [45]. Induced CD spectra (ICD) produced after the binding of achiral ligands to nucleic acids may be particularly informative in assessing the modes of binding (intercalation, groove binding) [46]. The addition of compounds 8, 9 and 15 caused a decrease in CD spectra of ctDNA at 275 nm and strong positive ICD bands (360–400 nm) that suggest minor groove binding to DNA. The binding of compounds 5 and 6 to ctDNA caused the appearance of bisignate ICD signals (360–400 nm) and negative ICD signals (305–360 nm), respectively (Figures 3 and S8, SI).

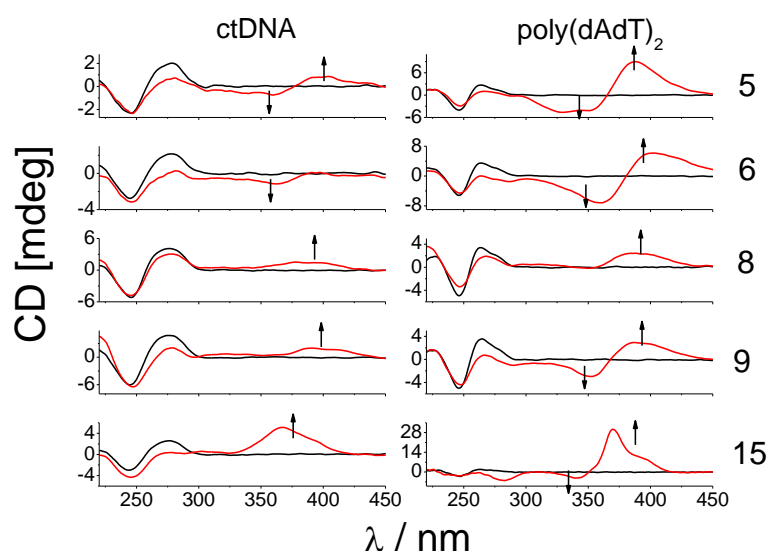


Figure 3. CD titrations of ctDNA and poly(dAdT)₂ ($c = 3.0 \times 10^{-5} \text{ mol dm}^{-3}$) with 5, 6, 8, 9 and 15 at molar ratios $r = [\text{compound}]/[\text{polynucleotide}] = 0.5$; (polynucleotide –, complex –), pH = 7.0, buffer sodium cacodylate, $I = 0.05 \text{ mol dm}^{-3}$.

Such changes in CD spectra suggest the binding of **5** inside the ctDNA groove, most probably in the form of a dimer. Negative ICD signals in a titration of **6** are indicative of intercalative binding where the ligand is oriented “parallel” to the long axis of adjacent base pairs. At ratios r higher than 0.3, compound **6** probably form aggregates along the DNA backbone [47].

The nitro group has a stronger electron-withdrawing effect on a given compound than chlorine. This could be the reason for different modes of binding of furane-benzothiazole derivatives with the nitro group and chlorine to ctDNA. However, the assessment of the substituent effects of both groups on the electronic properties of the rest of the molecule would require a quantitative description of changes in the electronic structure of these systems, which exceeds the scope of this work [48]. Surprisingly, almost all derivatives, regardless of whether they have a chlorine or nitro group in their structure, induced the formation of bisignate signals in the CD spectra of poly(dAdT)₂ (range 330–400 nm).

These changes can probably be attributed to the binding of compound dimer or higher-order aggregates inside of poly(dAdT)₂ groove or along the polynucleotide backbone. Only compound **8** exhibited similar changes with poly(dAdT)₂ as with ctDNA.

The most likely reason for this is a different amidine moiety on the benzazole heterocycle; while compounds **9** and **15** have imidazole moiety, **8** possesses isopropylamidine moiety that probably interferes with dimer formation.

In addition, only at the lowest ratio, $r = 0.1$, did compounds **9** and **15** induce changes in the CD spectra of poly(dAdT)₂ (significant positive ICD signals at 390 and 370 nm, respectively) such as with ctDNA.

Interestingly, compound **15**, which differs from compound **9** only by benzazole ring (benzimidazole **15** vs. benzothiazole **9**) caused the largest changes in the CD spectra of poly(dAdT)₂, a significant decrease in CD intensity of DNA at 262 nm, an appearance of strong negative CD signal at 282 nm and positive/negative CD bands with maxima at 340 and 368 nm (Figures 3 and S8, SI).

The zero-crossing point of the unsymmetric bisignate CD signal was at 352 nm, in good agreement with the absorption maximum of **15** (Figures 3 and S2, SI). The greatest magnitude of bisignate CD signal was at the ratio $r = 0.3$. A strong decrease in CD intensity of poly(dAdT)₂ in the range from 260 to 290 nm was probably not a consequence of the significant changes of the polynucleotide conformation but rather a uniform orientation of benzimidazole-furan chromophore transition moments with regard to DNA chiral axis which resulted in a negative ICD spectrum in this range. Due to strong changes in CD spectra of the alternating AT copolymer, poly(dAdT)₂ with **15**, we performed CD titration with non-alternating AT polynucleotide, poly dA-poly dT (Figure 4). The decrease in CD intensity of poly dA-poly dT at their maxima at 260 and 283 nm was smaller than with alternating AT polynucleotide. Unlike with alternating AT-polynucleotide, the addition of **15** to poly dA-poly dT solution did not cause the appearance of bisignate ICD signal but a significant positive ICD signal in the range from 345 to 408 nm, similar to the ICD signal obtained with ctDNA (Figure 4).

Although both of these polynucleotides belong to the B-DNA family, non-alternating poly dA-poly dT differs from a classical B-helix by a distinct secondary B structure characterized by a much narrower and deeper minor groove than that of poly(dAdT)₂ [49]. Such differentiation between ICD signals (range from 345–405 nm) of alternating and non-alternating AT-copolymers is probably the consequence of different binding possibilities inside the minor grooves (extent of hydrophobic interactions, the difference in electrostatic molecular potential). Most likely, compound **15** binds in the form of dimer to alternating poly(dAdT)₂ and in the form of a monomer inside the narrower minor groove of non-alternating poly dA-poly dT.

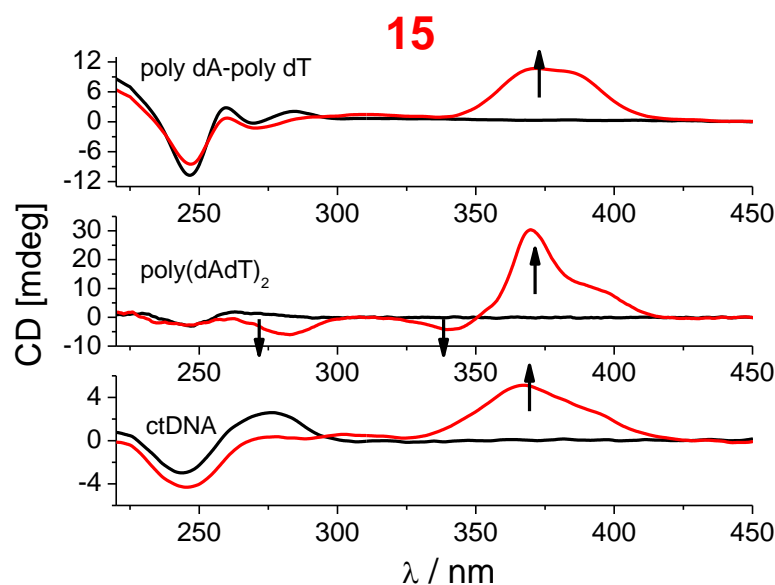


Figure 4. CD titrations of ctDNA, poly(dAdT)₂ and poly dA- poly dT ($c = 3.0 \times 10^{-5} \text{ mol dm}^{-3}$) with **15** at molar ratios $r = [\text{compound}]/[\text{polynucleotide}] = 0.5$; (polynucleotide –, complex –), pH = 7.0, buffer sodium cacodylate, $I = 0.05 \text{ mol dm}^{-3}$.

3. Materials and Methods

3.1. Chemistry

3.1.1. General

Melting points were determined by means of Original Kofler Mikroheitztisch apparatus (Reichert, Wien). ¹H NMR and ¹³C NMR spectra were recorded with the Bruker Avance DPX-300 or Bruker AV-600 using TMS as an internal standard. Chemical shifts are reported in parts per million (ppm) relative to TMS.

Elemental analyses for carbon, hydrogen and nitrogen were performed on Perkin-Elmer 2400 elemental analyzer. Analyses are indicated as symbols of elements, and the analytical results obtained are within 0.4% of the theoretical value.

3.1.2. General Method for Preparation of Compounds **4** and **7**

To a stirred suspension of disulfide **2a** (0.5 eq) in glycerol (1–1.5 g), the corresponding aldehyde **1a–1b** (1.0 eq) was added and heated at 165 °C for 45 min. The reaction mixture was cooled below 100 °C, quenched with ethanol and cooled in the refrigerator overnight. The resulting precipitate was collected by filtration, washed with ethanol and air-dried.

6-Cyano-2-[5-(4-nitrophenyl)furan-2-yl]benzothiazole 4.

Compound **4** was prepared from 5-(4-nitrophenyl)furan-2-carbaldehyde **1a** (0.109 g, 0.5 mmol) and bis(2-amino-5-cyanophenyl) disulfide **2a** (0.075 g, 0.25 mmol) to yield 0.144 g (83%) of beige powder; m.p. = 276–279 °C. ¹H NMR (600 MHz, DMSO-*d*₆) δ = 8.78 (d, J = 1.4 Hz, 1H, Ar-H), 8.36 (d, J = 8.9 Hz, 2H, Ar-H), 8.20 (d, J = 8.3 Hz, 1H, Ar-H), 8.12 (d, J = 8.8 Hz, 2H, Ar-H), 7.96 (dd, J = 8.4, 1.5 Hz, 1H, Ar-H), 7.70 (d, J = 3.8 Hz, 1H, Ar-H), 7.64 (d, J = 3.8 Hz, 1H, Ar-H). Anal. calc. for C₁₈H₁₀N₃O₃S: C, 62.24; H, 2.61; N, 12.10. Found: C, 62.13; H, 2.67; N, 12.04.

2-[5-(4-Chlorophenyl)furan-2-yl]-6-cyanobenzothiazole 7.

Compound **7** was prepared from 5-(4-chlorophenyl)furan-2-carbaldehyde **1b** (0.104 g, 0.5 mmol) and bis(2-amino-5-cyanophenyl) disulfide **2a** (0.075 g, 0.25 mmol) to yield 0.108 g (64%) of yellow powder; m.p. = 235–237 °C. ¹H NMR (600 MHz, DMSO-*d*₆) δ = 8.75 (d, J = 1.4 Hz, 1H, Ar-H), 8.17 (d, J = 8.4 Hz, 1H, Ar-H), 7.95 (dd, J = 8.4, 1.6 Hz, 1H, Ar-H), 7.90 (d, J = 8.6 Hz, 2H, Ar-H), 7.63 (d, J = 3.7 Hz, 1H, Ar-H), 7.59 (d, J = 8.6 Hz, 2H, Ar-H), 7.38 (d, J = 3.7 Hz, 1H, Ar-H). ¹³C NMR (150 MHz, DMSO-*d*₆) δ = 160.4, 156, 155.4, 147.2.

134.5, 133.6, 130.0, 129.2 (2C), 127.8, 127.5, 126.1 (2C), 123.3, 118.6, 116.1, 109.8, 107.5. Anal. calc. for C₁₈H₉ClN₂OS: C, 64.19; H, 2.69; N, 8.32. Found: C, 64.31; H, 2.60; N, 8.30.

3.1.3. General Method for Preparation of Compounds 5–6 and 8–9

To a stirred suspension of disulfides **2b–2c** (0.5 eq) in glycerol (1.5 g), the corresponding aldehyde **1a–1b** (1.0 eq) was added and heated at 165 °C for 45 min. The reaction mixture was cooled, diluted with water and made alkaline (pH 10–12) with 20% NaOH. The resulting free base was filtered, washed with water and dried.

The crude free base was suspended in 2-propanol and an excess of concentrated hydrochloric acid was added and stirred at room temperature for 1–2 h.

2-[5-(4-Nitrophenyl)furan-2-yl]-6-N-isopropilamidinobenzothiazole hydrochloride 5.

Compound **5** was prepared from 5-(4-nitrophenyl)furan-2-carbaldehyde **1a** (0.098 g, 0.45 mmol) and bis(2-amino-5-*N*-isopropilamidinophenyl) disulfide dihydrochloride dihydrate **2b** (0.112 g, 0.23 mmol). The obtained free base was suspended in 2-propanol (4 mL) and concentrated hydrochloric acid (0.125 mL) was added and stirred at room temperature for 1 h. After cooling overnight, the resulting precipitate was filtered, washed with diethyl-ether to yield 0.043 g (22%) of pale orange powder; m.p. = 201–206 °C. ¹H NMR (300 MHz, DMSO-*d*₆) δ = 9.44 (bs, 3H, NH_{amidine}), 8.63 (d, *J* = 1.6 Hz, 1H, Ar-H), 8.38 (d, *J* = 8.9 Hz, 2H, Ar-H), 8.25 (d, *J* = 8.6 Hz, 1H, Ar-H), 8.15 (d, *J* = 8.9 Hz, 2H, Ar-H), 7.87 (dd, *J* = 8.6, 1.7 Hz, 1H, Ar-H), 7.71 (d, *J* = 3.7 Hz, 1H, Ar-H), 7.67 (d, *J* = 3.8 Hz, 1H, Ar-H), 4.13–4.03 (m, 1H, CH), 1.31 (d, *J* = 6.3 Hz, 6H, CH₃). ¹³C NMR (75 MHz, DMSO-*d*₆) δ = 161.3, 159.4, 155.9, 153.8, 148.5, 146.8, 134.5, 133.9, 126.9, 126.5, 125.1 (2C), 124.6 (2C), 123.5, 122.7, 116.1, 113.1, 45.2, 21.4 (2C). Anal. calc. for C₂₁H₁₉ClN₄O₃S: C, 56.95; H, 4.32; N, 12.65. Found: C, 57.03; H, 4.28; N, 12.61.

6-(4,5-Dihydro-1H-imidazol-2-yl)-2-[5-(4-nitrophenyl)furan-2-yl]benzothiazole hydrochloride 6.

Compound **6** was prepared from 5-(4-nitrophenyl)furan-2-carbaldehyde **1a** (0.110 g, 0.50 mmol) and bis [2-amino-5-(4,5-Dihydro-1H-imidazol-2-yl)phenyl] disulfide dihydrochloride dihydrate **2c** (0.123 g, 0.25 mmol). The obtained free base was suspended in 2-propanol (15 mL) and concentrated hydrochloric acid (0.150 mL) was added and stirred at room temperature for 2 h. After cooling overnight, the resulting precipitate was filtered, washed with diethyl-ether to yield 0.120 g (56%) of pale orange powder; m.p. = 287–292 °C. ¹H NMR (300 MHz, DMSO-*d*₆) δ = 10.82 (s, 2H, NH_{amidine}), 8.86 (d, *J* = 1.5 Hz, 1H, Ar-H), 8.36 (d, *J* = 8.9 Hz, 2H, Ar-H), 8.29 (d, *J* = 8.5 Hz, 1H, Ar-H), 8.16–8.10 (m, 3H, Ar-H), 7.72 (d, *J* = 3.7 Hz, 1H, Ar-H), 7.66 (d, *J* = 3.7 Hz, 1H, Ar-H), 4.06 (s, 4H, CH₂). Anal. calc. for C₂₀H₁₅ClN₄O₃S: C, 56.27; H, 3.54; N, 13.12. Found: C, 56.20; H, 3.67; N, 13.18.

2-[5-(4-Chlorophenyl)furan-2-yl]-6-N-isopropilamidinobenzothiazole hydrochloride 8.

Compound **8** was prepared from 5-(4-chlorophenyl)furan-2-carbaldehyde **1b** (0.103 g, 0.5 mmol) and bis(2-amino-5-*N*-isopropilamidinophenyl) disulfide dihydrochloride dihydrate **2b** (0.122 g, 0.25 mmol). The obtained free base was suspended in 2-propanol (3 mL) and concentrated hydrochloric acid (0.100 mL) was added and stirred at room temperature for 2 h. After cooling overnight, the resulting precipitate was filtered, washed with diethyl-ether to yield 0.061 g (28%) of yellow powder; m.p. = 204–208 °C. ¹H NMR (300 MHz, DMSO-*d*₆) δ = 9.84–9.40 (m, 3H, NH_{amidine}), 8.64 (d, *J* = 1.5 Hz, 1H, Ar-H), 8.20 (d, *J* = 8.6 Hz, 1H, Ar-H), 7.92–7.86 (m, 3H, Ar-H), 7.62–7.57 (m, 3H, 3H, Ar-H), 7.40 (d, *J* = 3.6 Hz, 1H, Ar-H), 4.26–4.14 (m, 1H, CH), 1.32 (d, *J* = 6.3 Hz, 6H, CH₃). ¹³C NMR (75 MHz, DMSO-*d*₆) δ = 161.4, 159.7, 156.1, 155.1, 147.2, 133.8, 133.5, 129.3 (2C), 127.7, 126.9, 126.0 (2C), 125.9, 123.5, 122.4, 116.0, 110.0, 45.3, 21.3 (2C). Anal. calc. for C₂₁H₁₉Cl₂N₃OS: C, 58.34; H, 4.43; N, 9.72. Found: C, 58.38; H, 4.38; N, 9.72.

2-[5-(4-Chlorophenyl)furan-2-yl]-6-(4,5-Dihydro-1H-imidazol-2-yl)benzothiazole hydrochloride 9.

Compound **9** was prepared from 5-(4-chlorophenyl)furan-2-carbaldehyde **1b** (0.103 g, 0.5 mmol) and bis[2-amino-5-(4,5-Dihydro-1H-imidazol-2-yl)phenyl] disulfide dihydrochloride dihydrate **2c** (0.123 g, 0.25 mmol). The obtained free base was suspended in 2-propanol (10 mL) and concentrated hydrochloric acid (0.125 mL) was added and stirred at room temperature for 1 h. After cooling overnight, the resulting precipitate was filtered, washed

with diethyl-ether to yield 0.110 g (53%) of yellow powder powder; m.p. = 293–297 °C. ^1H NMR (600 MHz, DMSO- d_6) δ = 10.87 (s, 2H, $\text{NH}_{\text{amidine}}$), 8.88 (d, J = 1.6 Hz, 1H, Ar-H), 8.25 (d, J = 8.5 Hz, 1H, Ar-H), 8.14 (dd, J = 8.6, 1.7 Hz, 1H, Ar-H), 7.91 (d, J = 8.6 Hz, 2H, Ar-H), 7.64 (d, J = 3.7 Hz, 1H, Ar-H), 7.59 (d, J = 8.5 Hz, 2H, Ar-H), 7.40 (d, J = 3.7 Hz, 1H, Ar-H), 4.05 (s, 4H, CH_2). ^{13}C NMR (75 MHz, DMSO- d_6) δ = 164.2, 160.3, 156.8, 155.3, 146.9, 134.1, 133.5, 129.2 (2C), 127.5, 126.9, 125.9 (2C), 123.7, 122.8, 118.5, 116.3, 110.0, 44.4 (2C). Anal. calc. for $\text{C}_{20}\text{H}_{15}\text{Cl}_2\text{N}_3\text{OS}$: C, 57.70; H, 3.63; N, 10.09. Found: C, 57.63; H, 3.65; N, 10.18.

3.1.4. General Method for Preparation of Compounds 10–15

Solution of equimolar amounts of aldehydes **1a–1b**, corresponding derivatives **3a–3c**, and *p*-benzoquinone in absolute ethanol, was refluxed for 2.5–4 h. After the reaction mixture was cooled to room temperature, the crude product was filtered off and washed with diethyl ether or was separated by column chromatography on SiO_2 .

5(6)-Cyano-2-[5-(4-nitrophenyl)furan-2-yl]benzimidazole **10**.

Compound **10** was prepared from 5-(4-nitrophenyl)furan-2-carbaldehyde **1a** (0.60 g, 2.70 mmol), 3,4-diaminobenzonitrile **3a** (0.37 g, 2.70 mmol) and *p*-benzoquinone (0.29 g, 2.70 mmol) in absolute ethanol (15 mL) after refluxing for 4 h. Resulting product was separated by column chromatography on SiO_2 using dichloromethane as eluent to yield 0.15 g (15%) of red powder; m.p. 242–246 °C. ^1H NMR (600 MHz, DMSO- d_6) δ = 8.64 (s, 1H, Ar-H), 8.34 (d, J = 9.0 Hz, 2H, Ar-H), 8.13 (d, J = 9.0 Hz, 2H, Ar-H), 7.58 (d, J = 1.7 Hz, 1H, Ar-H), 7.54 (d, J = 3.7 Hz, 1H, Ar-H), 7.38 (d, J = 3.7 Hz, 1H, Ar-H), 7.35 (dd, J = 8.4, 1.8 Hz, 1H, Ar-H). ^{13}C NMR (75 MHz, DMSO- d_6) δ = 153.9, 149.0, 147.1, 146.8, 135.5, 135.0, 132.6, 132.2, 125.5, 125.0, 121.2, 120.8, 119.6, 114.8, 113.1, 96.6. Found: Anal. calc. for $\text{C}_{18}\text{H}_{10}\text{N}_4\text{O}_3$: C, 65.45; H, 3.05; N, 16.96. Found: C, 65.55; H, 3.08; N, 16.95.

2-[5-(4-Nitrophenyl)furan-2-yl]-5(6)-*N*-isopropylamidinobenzimidazole hydrochloride **11**.

Compound **11** was prepared from 5-(4-nitrophenyl)furan-2-carbaldehyde **1a** (0.30 g, 1.40 mmol), 4-(*N*-isopropylamido)-1,2-phenylenediamine hydrochloride **3b** (0.32 g, 1.40 mmol) and *p*-benzoquinone (0.15 g, 1.40 mmol) in absolute ethanol (15 mL) after refluxing for 2.5 h to yield 0.49 g (85%) of dark yellow powder; m.p. > 270 °C. ^1H NMR (300 MHz, DMSO- d_6) δ = 13.88 (s, 1H, $\text{NH}_{\text{benzim.}}$), 9.56 (s, 2H, $\text{NH}_{\text{amidine}}$), 9.42 (s, 1H, $\text{NH}_{\text{amidine}}$), 9.01 (s, 1H, Ar-H), 8.39 (d, J = 8.9 Hz, 2H, Ar-H), 8.22 (d, J = 8.9 Hz, 2H, Ar-H), 7.87–7.76 (m, 1H, Ar-H), 7.61–7.56 (m, 3H, Ar-H), 4.11–4.05 (m, 1H, NH), 1.31 (d, J = 6.3 Hz, 6H, 2CH_3). ^{13}C NMR (150 MHz, DMSO- d_6) δ = 162.4, 146.5, 146.0, 135.1, 124.8, 124.5, 112.5, 45.0, 21.3 (2C). Anal. calc. for $\text{C}_{21}\text{H}_{20}\text{ClN}_5\text{O}_3$: C, 59.23; H, 4.73; N, 16.44. Found: C, 59.22; H, 4.75; N, 16.42.

5(6)-(4,5-Dihydro-1*H*-imidazol-2-yl)-2-[5-(4-nitrophenyl)furan-2-yl]benzimidazole hydrochloride **12**.

Compound **12** was prepared from 5-(4-nitrophenyl)furan-2-carbaldehyde **1a** (0.30 g, 1.40 mmol), 4-(4,5-dihydro-1*H*-imidazol-2-yl)-1,2-phenylenediamine hydrochloride **3c** (0.33 g, 1.40 mmol) and *p*-benzoquinone (0.29 g, 2.70 mmol) in absolute ethanol (10 mL) after refluxing for 3 h to yield 0.54 g (96%) of dark green powder; m.p. > 270 °C. ^1H NMR (300 MHz, DMSO- d_6) δ = 14.05 (s, 1H, $\text{NH}_{\text{benzim.}}$), 13.94 (s, 1H, $\text{NH}_{\text{benzim.}}$), 10.66 (s, 2H, $\text{NH}_{\text{amidine}}$), 10.61 (s, 2H, $\text{NH}_{\text{amidine}}$), 8.37 (d, J = 8.9 Hz, 2H, Ar-H), 8.33–8.27 (m, 1H, Ar-H), 8.21 (d, J = 8.9 Hz, 1H, Ar-H), 8.17–8.10 (m, 1H, Ar-H), 7.96–7.78 (m, 4H, Ar-H), 7.63–7.53 (m, 4H, Ar-H), 4.04 (s, 8H, CH_2). ^{13}C NMR (75 MHz, DMSO- d_6) δ = 146.5, 145.7, 135.0, 124.9, 124.8 (2C), 124.5 (2C), 124.3, 123.8, 115.6, 112.5, 44.21 (2C). Anal. calc. for $\text{C}_{20}\text{H}_{16}\text{ClN}_5\text{O}_3$: C, 58.61; H, 3.94; N, 17.09. Found: C, 58.44; H, 3.99; N, 17.43.

2-[5-(4-Chlorophenyl)furan-2-yl]-5(6)-cyanobenzimidazole **13**.

Compound **13** was prepared from 5-(4-chlorophenyl)furan-2-carbaldehyde **1b** (0.50 g, 2.40 mmol), 3,4-diaminobenzonitrile **3a** (0.32 g, 2.40 mmol) and *p*-benzoquinone (0.26 g, 2.40 mmol) in absolute ethanol (10 mL) after refluxing for 3 h to yield 0.27 g (36%) of green powder; m.p. 242–246 °C. ^1H NMR (300 MHz, DMSO- d_6) δ = 13.57 (bs, 1H, $\text{NH}_{\text{benzim.}}$), 8.58 (s, 1H, Ar-H), 7.97 (d, J = 8.4 Hz, 2H, Ar-H), 7.90 (d, J = 8.6 Hz, 2H, Ar-H), 7.61–7.54 (m,

4H, Ar-H). ^{13}C NMR (150 MHz, DMSO- d_6) δ = 144.1, 132.9, 129.3, 129.1, 129.1 (2C), 128.2, 126.7, 125.8 (2C), 119.9, 115.6, 109.2, 107.4, 104.1. Anal. calc. for $\text{C}_{18}\text{H}_{10}\text{ClN}_3\text{O}$: C, 67.61; H, 3.15; N, 13.14. Found: C, 67.60; H, 3.13; N, 13.17.

2-[5-(4-Chlorophenyl)furan-2-yl]-5(6)-isopropilamidinobenzimidazole hydrochloride 14.

Compound **14** was prepared from 5-(4-chlorophenyl)furan-2-carbaldehyde **1b** (0.30 g, 1.40 mmol), 4-(*N*-isopropylamidino)-1,2-phenylenediamine hydrochloride **3b** (0.32 g, 1.40 mmol) and *p*-benzoquinone (0.15 g, 1.40 mmol) in absolute ethanol (10 mL) after refluxing for 3 h to yield 0.13 g (23%) of light grey powder; m.p. 242–246 °C. ^1H NMR (300 MHz, DMSO- d_6) δ = 13.73 (bs, 1H, $\text{NH}_{\text{benzim.}}$), 9.48 (bs, 3H, $\text{NH}_{\text{amidine}}$), 8.00 (s, 1H, Ar-H), 7.98 (d, J = 8.5 Hz, 2H, Ar-H), 7.78 (d, J = 8.3 Hz, 1H, Ar-H), 7.60 (d, J = 8.7 Hz, 2H, Ar-H), 7.56 (d, J = 8.6 Hz, 1H, Ar-H), 7.47 (d, J = 3.6 Hz, 1H, Ar-H), 7.32 (d, J = 3.6 Hz, 1H, Ar-H), 4.15–4.02 (m, 1H, CH), 1.31 (d, J = 6.3 Hz, 6H, CH_3). ^{13}C NMR (75 MHz, DMSO- d_6) δ = 162.9, 154.2, 144.9, 133.3, 129.6 (2C), 128.7, 126.3 (2C), 123.4, 114.8, 109.6, 45.5, 21.8 (2C). Anal. calc. for $\text{C}_{21}\text{H}_{20}\text{Cl}_2\text{N}_4\text{O}$: C, 60.73; H, 4.85; N, 13.49. Found: C, 60.72; H, 4.87; N, 13.48.

2-[5-(4-Chlorophenyl)furan-2-yl]-5(6)-(4,5-dihydro-1H-imidazol-2-yl)benzimidazole hydrochloride 15.

Compound **15** was prepared from 5-(4-chlorophenyl)furan-2-carbaldehyde **1b** (0.30 g, 1.40 mmol), 4-(4,5-dihydro-1H-imidazol-2-yl)-1,2-phenylenediamine hydrochloride **3c** (0.34 g, 1.40 mmol) and *p*-benzoquinone (0.15 g, 1.40 mmol) in absolute ethanol (10 mL) after refluxing for 3 h to yield 0.54 g (96%) of grey powder; m.p. 262–269 °C. ^1H NMR (300 MHz, DMSO- d_6) δ = 10.83 (bs, 2H, $\text{NH}_{\text{amidine}}$), 8.35 (s, 1H, Ar-H), 7.99 (d, J = 8.6 Hz, 2H, Ar-H), 7.87 (d, J = 8.6 Hz, 1H, Ar-H), 7.81 (d, J = 8.5 Hz, 1H, Ar-H), 7.60 (d, J = 8.6 Hz, 2H, Ar-H), 7.50 (d, J = 3.6 Hz, 1H, Ar-H), 7.32 (d, J = 3.6 Hz, 1H, Ar-H), 4.03 (s, 4H, CH_2). ^{13}C NMR (75 MHz, DMSO- d_6) δ = 165.7, 154.4, 144.7, 133.4, 129.5 (2C), 128.7, 126.3 (2C), 123.2, 116.1, 116.0, 115.1, 109.6 (2C), 44.7 (2C). Anal. calc. for $\text{C}_{20}\text{H}_{16}\text{Cl}_2\text{N}_4\text{O}$: C, 60.16; H, 4.04; N, 14.03. Found: C, 60.18; H, 4.03; N, 14.04.

3.1.5. General Method for Preparation of Compounds 17–22

Solution of equimolar amounts of heteroaromatic aldehydes **1a–1b**, the corresponding derivatives **16a–16c**, and a few drops of piperidine in absolute ethanol, was refluxed for 1 h. After the reaction mixture was cooled to room temperature, the crude product was filtered off and recrystallized from ethanol or was separated by column chromatography on SiO_2 .

(E)-2-(Benzimidazol-2-yl)-3-[5-(4-nitrophenyl)furan-2-yl]acrylonitrile 17 [50].

Compound **17** was prepared from 5-(4-nitrophenyl)furan-2-carbaldehyde **1a** (1.38 g, 6.00 mol) and 2-cyanomethylbenzimidazole **16a** (1.00 g, 6.00 mol) in absolute ethanol (10 mL) after refluxing for 2 h. Resulting product was filtered off and recrystallized from ethanol to yield 1.78 g (84%) of orange powder; m.p. 273–274 °C. ^1H NMR (300 MHz, DMSO- d_6) δ = 13.10 (s, 1H, $\text{NH}_{\text{benzim.}}$), 8.39 (d, 2H, J = 8.9 Hz, Ar-H), 8.20 (s, 1H, Ar-H), 8.14 (d, 2H, J = 8.8 Hz, Ar-H), 7.69 (d, 1H, J = 8.7 Hz, Ar-H), 7.68 (d, 1H, J = 3.7 Hz, Ar-H), 7.54 (d, 1H, J = 8.7 Hz, Ar-H), 7.46 (d, 1H, J = 3.8 Hz, Ar-H), 7.30–7.23 (m, 2H, Ar-H). ^{13}C NMR (75 MHz, DMSO- d_6) δ = 154.9, 150.4, 147.7, 147.4, 144.0, 135.4, 135.0, 130.0, 125.7, 125.1, 124.2, 122.8, 119.6, 116.8, 113.8, 112.0, 99.0. Anal. calc. for $\text{C}_{20}\text{H}_{12}\text{N}_4\text{O}_3$: C, 67.41; H, 3.39; N, 15.72. Found: C, 67.66; H, 3.58; N, 15.40.

(E,Z)-2-(5(6)-Nitrobenzimidazol-2-yl)-3-[5-(4-nitrophenyl)furan-2-yl]acrylonitrile 18.

Compound **18** was prepared from 5-(4-nitrophenyl)furan-2-carbaldehyde **1a** (0.07 g, 0.32 mmol) and 2-cyanomethyl-5(6)-nitrobenzimidazole **16b** (0.07 g, 0.32 mmol) in absolute ethanol (5 mL) after refluxing for 1 h. The resulting product was separated by column chromatography on SiO_2 using dichloromethane/methanol as eluent to yield 0.05 g (41%) of orange powder; m.p. > 300 °C. **a:** ^1H NMR (300 MHz, DMSO- d_6) δ = 13.70 (s, 1H, $\text{NH}_{\text{benzim.}}$), 8.41 (s, 1H, Ar-H), 8.33 (d, J = 8.9 Hz, 2H, Ar-H), 8.24 (s, 1H, Ar-H), 8.14–8.06 (m, 3H, Ar-H), 7.72 (d, J = 8.8 Hz, 1H, Ar-H), 7.65 (d, J = 3.9 Hz, 1H, Ar-H), 7.51 (d, J = 3.8 Hz, 1H, Ar-H). **b:** ^1H NMR (300 MHz, DMSO- d_6) δ = 13.70 (s, 1H, $\text{NH}_{\text{benzim.}}$), 8.60 (s, 1H, Ar-H), 8.33 (d, J = 8.9 Hz, 2H, Ar-H), 8.14–8.06 (m, 3H, Ar-H), 7.94 (s, 1H, Ar-H), 7.85 (d, J = 8.9 Hz, 1H,

Ar-H), 7.69 (d, $J = 3.9$ Hz, 1H, Ar-H), 7.56 (d, $J = 3.8$ Hz, 1H, Ar-H). ^{13}C NMR (75 MHz, DMSO- d_6) $\delta = 155.6, 150.1, 147.5, 143.6, 134.7, 131.9, 125.8$ (2C), 125.0 (2C), 124.4, 116.5, 113.9, 97.6. Anal. calc. for $\text{C}_{20}\text{H}_{11}\text{N}_5\text{O}_5$: C, 59.85; H, 2.76; N, 17.45. Found: C, 59.86; H, 2.78; N, 17.44.

(E)-2-(Benzothiazol-2-yl)-3-[5-(4-nitrophenyl)furan-2-yl]acrylonitrile **19**.

Compound **19** was prepared from 5-(4-nitrophenyl)furan-2-carbaldehyde **1a** (0.13 g, 0.57 mmol) and 2-cyanomethylbenzothiazole **16c** (0.10 g, 0.57 mmol) in absolute ethanol (7 mL) after refluxing for 1 h and recrystallization from ethanol to yield 0.19 g (90%) of orange powder; m.p. 240–242 °C. ^1H NMR (300 MHz, DMSO- d_6) $\delta = 8.30$ (d, $J = 8.7$ Hz, 2H, Ar-H), 8.22 (s, 1H, Ar-H), 8.12 (d, $J = 7.9$ Hz, 1H, Ar-H), 8.07 (d, $J = 8.7$ Hz, 2H, Ar-H), 8.01 (d, $J = 8.0$ Hz, 1H, Ar-H), 7.62 (d, $J = 3.7$ Hz, 1H, Ar-H), 7.54 (t, $J = 7.1$ Hz, 1H, Ar-H), 7.52 (d, $J = 3.8$ Hz, 1H, Ar-H), 7.46 (t, $J = 7.5$ Hz, 1H, Ar-H). ^{13}C NMR (75 MHz, DMSO- d_6) $\delta = 163.1, 155.8, 153.6, 150.2, 147.7, 135.0, 134.8, 132.1, 127.6, 126.6, 126.0$ (2C), 125.0 (3C), 123.5, 122.9, 116.8, 113.9, 101.7. Anal. calc. for $\text{C}_{20}\text{H}_{11}\text{N}_3\text{O}_3\text{S}$: C, 64.33; H, 2.97; N, 11.25. Found: C, 64.31; H, 2.98; N, 11.24.

(E)-2-(Benzimidazol-2-yl)-3-[5-(4-chlorophenyl)furan-2-yl]acrylonitrile **20**.

Compound **20** was prepared from 5-(4-chlorophenyl)furan-2-carbaldehyde **1b** (1.24 g, 6.00 mmol) and 2-cyanomethylbenzimidazole **16a** (1.00 g, 6.00 mmol) in absolute ethanol (20 mL) after refluxing for 2 h. Resulting product was filtered off and recrystallized from ethanol to yield 1.27 g (61%) of orange powder; m.p. 292–294 °C. ^1H NMR (300 MHz, DMSO- d_6) $\delta = 13.00$ (s, 1H, $\text{NH}_{\text{benzimid.}}$), 8.15 (s, 1H, Ar-H), 7.94 (d, 2H, $J = 8.6$ Hz, Ar-H), 7.84 (d, 1H, $J = 8.8$ Hz, Ar-H), 7.63 (d, 2H, $J = 8.6$ Hz, Ar-H), 7.50 (d, 1H, $J = 8.8$ Hz, Ar-H), 7.42 (d, 1H, $J = 3.7$ Hz, Ar-H), 7.40 (d, 1H, $J = 3.7$ Hz, Ar-H), 7.24 (brs, 2H, Ar-H). ^{13}C NMR (75 MHz, DMSO- d_6) $\delta = 156.3, 149.1, 148.0, 144.0, 134.2, 130.2, 129.8$ (2C), 128.2, 126.7 (2C), 125.7, 123.0, 119.5, 117.0, 112.0, 110.8, 109.6, 97.5. Anal. calc. for $\text{C}_{20}\text{H}_{12}\text{ClN}_3\text{O}$: C, 69.47; H, 3.50; N, 12.15. Found: C, 69.20; H, 3.33; N, 12.45.

(E,Z)-3-[5-(4-Chlorophenyl)furan-2-yl]-2-(5(6)-nitrobenzimidazol-2-yl)acrylonitrile **21**.

Compound **21** was prepared from 5-(4-chlorophenyl)furan-2-carbaldehyde **1b** (0.10 g, 0.48 mmol) and 2-cyanomethyl-5(6)-nitrobenzimidazole **16b** (0.10 g, 0.48 mmol) in absolute ethanol (5 mL) after refluxing for 1 h. Resulting product was separated by column chromatography on SiO_2 using dichloromethane/methanol as eluent to yield 0.07 g (35%) of orange powder; m.p. > 300 °C. **a**: ^1H NMR (600 MHz, DMSO- d_6) $\delta = 13.62$ (s, 1H, $\text{NH}_{\text{benzimid.}}$), 8.42 (s, 1H, Ar-H), 8.21 (s, 1H, Ar-H), 8.09 (dd, $J = 8.9, 2.2$ Hz, 1H, Ar-H), 7.90 (d, $J = 8.6$ Hz, 2H, Ar-H), 7.72 (d, $J = 8.8$ Hz, 1H, Ar-H), 7.57 (d, $J = 8.6$ Hz, 2H, Ar-H), 7.45 (d, $J = 3.7$ Hz, 1H, Ar-H), 7.41 (d, $J = 3.7$ Hz, 1H, Ar-H). **b**: ^1H NMR (600 MHz, DMSO- d_6) $\delta = 13.62$ (s, 1H, $\text{NH}_{\text{benzimid.}}$), 8.454 (s, 1H, Ar-H), 8.22 (s, 1H, Ar-H), 7.90–7.89 (m, 1H, Ar-H), 7.86 (s, 1H, Ar-H), 7.59–7.57 (m, 1H, Ar-H), 7.39 (d, $J = 8.6$ Hz, 2H, Ar-H), 7.32 (d, $J = 8.6$ Hz, 2H, Ar-H), 7.29 (d, $J = 3.7$ Hz, 1H, Ar-H). ^{13}C NMR (75 MHz, DMSO- d_6) $\delta = 157.1, 148.9, 143.5, 134.5, 132.1, 129.8$ (2C), 127.9, 126.8 (2C), 124.7, 116.7, 111.1, 96.1. Anal. calc. for $\text{C}_{20}\text{H}_{11}\text{ClN}_4\text{O}_3$: C, 61.47; H, 2.84; N, 14.34. Found: C, 61.46; H, 2.86; N, 14.32.

(E)-2-(Benzothiazol-2-yl)-3-[5-(4-chlorophenyl)furan-2-yl]acrylonitrile **22**.

Compound **22** was prepared from 5-(4-chlorophenyl)furan-2-carbaldehyde **1b** (0.12 g, 0.57 mmol) and 2-cyanomethylbenzothiazole **13** (0.10 g, 0.57 mmol) in absolute ethanol (7 mL) after refluxing for 1 h and recrystallization from ethanol to yield 0.17 g (81%) of yellow powder; m.p. 190–192 °C. ^1H NMR (300 MHz, DMSO- d_6) $\delta = 8.24$ (s, 1H, Ar-H), 8.16 (d, $J = 8.0$ Hz, 1H, Ar-H), 8.05 (d, $J = 7.9$ Hz, 1H, Ar-H), 7.94 (d, $J = 8.6$ Hz, 2H, Ar-H), 7.62 (d, $J = 8.7$ Hz, 2H, Ar-H), 7.58–7.54 (m, 1H, Ar-H), 7.52 (d, $J = 3.7$ Hz, 1H, Ar-H), 7.51–7.46 (m, 1H, Ar-H), 7.44 (d, $J = 3.7$ Hz, 1H, Ar-H). ^{13}C NMR (75 MHz, DMSO- d_6) $\delta = 163.9, 157.7, 154.0, 149.3, 135.2, 135.0, 132.6, 130.3$ (2C), 128.4, 128.0, 127.3 (2C), 126.9, 126.1, 123.7, 123.3, 117.4, 111.6, 100.5. Anal. calc. for $\text{C}_{20}\text{H}_{11}\text{ClN}_2\text{OS}$: C, 66.21; H, 3.06; N, 7.72. Found: C, 66.20; H, 3.08; N, 7.73.

3.2. Pharmacological/Biological Assays

3.2.1. Antitumor Activity in 2D and 3D Cell Culture Assays In Vitro

Test compounds.

Doxorubicin was purchased from Apollo (BID0120; Opelika, AL, USA), staurosporine was purchased from Biotrend (BS0188; Zurich, SUI, Switzerland) and vandetanib was purchased from Selleckchem (S1046, Houston, TX, USA). Test compounds were synthesized by a research group at the Department of Organic Chemistry, Faculty of Chemical Engineering and Technology, University of Zagreb. Mother plates (96-well-V plates, polypropylene, Greiner Bio-one, Cat. 651201) with serial dilutions of compounds in pure DMSO were prepared from 10 mM DMSO stock solutions on Janus automatic pipetting workstation (Perkin-Elmer). Compounds were diluted 1:3. We transferred 500 nL (for 2D cell culture) or 400 nL (for 3D cell culture) of the compound from a mother plate to test plate by using Mosquito (TTP labtech). DMSO percentage in test concentrations was 0.5–1.0%. Starting concentration of the test compounds and standard compound doxorubicin was 50 μ M (2D cell culture) or 100 μ M (3D cell culture). Starting concentration of staurosporine was 10 μ M in both, 2D and 3D cell culture assays, while starting concentration of vandetanib was 25 μ M (2D cell culture) or 50 μ M (3D cell culture).

Cell cultures.

Human lung cancer cell lines A549 (ATCC CCL-185), HCC827 (ATCC CRL-2868) and NCI-H358 (ATCC CRL-5807) and human lung fibroblast cell line MRC-5 (ATCC CCL-171) were purchased from American Type Culture Collection (ATCC, Manassas, VA, USA). Cells were maintained in appropriate medium, recommended by supplier medium, supplemented with 10% heat inactivated fetal bovine serum and penicillin/streptomycin, in an incubator (INCO2, Memmert, Germany) in a humidified atmosphere of 5% CO₂ and 95% O₂ at 37 °C.

High-Throughput 2D and 3D Drug Screening Setup.

2D cell culture assay.

Cells were grown in 96-well cell star polystyrene plates. We seeded 10,000 cells/well in wells 4 h prior to the treatment with different compounds concentrations and incubated for 72 h. A cell viability assay was performed according to the manufacturer's instructions, using CellTiter 96 aqueous solution, MTS kit (Promega, Madison, WI, USA). After 0.5–2 h of cell incubation with MTS in 2D cell culture, the plates were read using PE EnVision absorbance at 490 nm. The results for each of the tested compounds are reported as growth percentages from two independent concentrations curves compared with the untreated control cells after drug exposure.

3D cell culture assay.

Cells were grown in 96-well Perfecta 3D hanging drop plates 5000 cell/well for 4 days until spheres were formed (and checked under the microscope). After sphere formation cells were treated with compounds followed by 72 h incubation. Cell viability assay was performed according to the manufacturer's instructions, using CellTiter GLO 3D for 3D cell culture (Promega); cell incubation was 5 min on the shaker followed by 25 min incubation in the dark. Plates were read using PE EnVision luminescence.

The results for each of the tested compounds are reported as growth percentages from two independent concentrations curves compared with the untreated control cells after drug exposure.

BrdU Proliferation Assay.

Proliferation assay was performed using Cell Proliferation ELISA, BrdU (Sigma, St. Louis, MO, USA). Briefly, 48 h hours after compound addition, 10 μ M of BrdU was added to each well and incubated for the following 24 h. After incubation, a single cell suspension was made for 3D cell culture in the new 96-well plate. Plates were centrifuged and supernatants were removed from each plate (for 2D and 3D cell culture) followed by 60 min incubation at 60 °C. The rest of the proliferation assay was performed according to the manufacturer's instructions.

Statistical Analysis.

Calculation of IC₅₀ data, curves and QC analysis was performed by using Excel tools and GraphPadPrism software (La Jolla, CA, USA), v. 5.03. In brief, individual concentration–effect curves are generated by plotting the logarithm of the tested concentration of tested compounds (X) versus corresponding percent inhibition values (Y) using least squares (ordinary) fit. Best fit IC₅₀ values are calculated using Log(inhibitor) versus normalized response–variable slope equation, where $Y = 100 / (1 + 10((\text{LogIC}_{50} - X) \times \text{HillSlope}))$. QC criteria parameters (Z', S:B, R2, HillSlope) were checked for every IC₅₀ curve.

3.2.2. In Vitro Antimicrobial Activity

Materials.

In addition to synthesized compounds, standard antibiotics ampicillin, ceftazidime, ciprofloxacin, gentamycin and voriconazole from USP were tested. Bacterial strains tested were Gram-negative *Escherichia coli* ATCC 25922 strain and Gram-positive *Staphylococcus aureus* ATCC 29213 strain. *Saccharomyces cerevisiae* ATCC 7752 strain was tested as a eukaryotic model organism. Synthesized compounds were prepared as 10 mM DMSO solutions and tested in the final concentration range of 100–0.2 μM. Standard antibiotics were prepared as 5 mg/mL DMSO solutions and tested in the final concentration range of 64–0.125 μg/mL.

Methods.

Broth microdilution testing was performed according to CLSI (Clinical Laboratory Standards Institute) guidelines. MIC (minimal inhibitory concentration) value was defined as the last tested concentration of compound at which there is no visible growth of bacteria. Inoculums for each microorganism were prepared using the direct colony suspension method where broth solutions that achieved turbidity equivalent to 0.5 McFarland standard were additionally diluted 100x with Ca adjusted MH media (Becton Dickinson). All test plates were incubated for 16–24h at 37 °C. MIC values for reference antibiotics against quality control strains were used for confirming the validity of the screen. Clinical and Laboratory Standards Institute (CLSI) guidelines. Methods for dilution antimicrobial susceptibility tests for bacteria that grow aerobically M07, 11th edition, 2018. and Clinical and Laboratory Standards Institute (CLSI) guidelines. Performance standards for antimicrobial susceptibility testing M100, 28th edition, 2018.

3.2.3. DNA Binding Study

All compounds were soluble in water (**5**, **8**, and **15** in $c = 3 \times 10^{-3} \text{ mol dm}^{-3}$, **6** and **9** in $c = 1.72 \times 10^{-3} \text{ mol dm}^{-3}$ and $1.32 \times 10^{-3} \text{ mol dm}^{-3}$). Due to the small aggregation of **6** and **9** in water, a stock solution was also prepared in DMSO ($c = 3 \times 10^{-3} \text{ mol dm}^{-3}$) to check the dependence of UV/Vis changes on concentration increase.

All other experiments with **5**, **6**, **8**, **9** and **15** ($c = 3 \times 10^{-3} \text{ mol dm}^{-3}$) were performed by adding small aliquots of aqueous stock solution to buffer solutions (0.05 M Na cacodylate) at 25 °C using appropriate 1cm path quartz cuvettes. Absorption maxima and corresponding molar extinction coefficients (ϵ) are given in Table S1 and Figures S1 and S2. The UV/vis spectra were recorded on a Varian Cary 100 Bio spectrophotometer, CD spectra on JASCO J815 spectrophotometer and fluorescence spectra on a Varian Cary Eclipse spectrophotometer.

Calf thymus ctDNA, poly(dAdT)₂ and poly dA–poly dT were purchased in Sigma-Aldrich and dissolved in Na-cacodylate buffer, $I = 0.05 \text{ mol dm}^{-3}$, pH = 7. The ctDNA was additionally sonicated and filtered through a 0.45 μm filter [51]. Polynucleotide concentration was determined spectroscopically as the concentration of phosphates [52]. Spectrophotometric titrations were performed at pH = 7 ($I = 0.05 \text{ mol dm}^{-3}$, sodium cacodylate buffer) by adding portions of polynucleotide solution into the solution of the studied compound for fluorimetric experiments and CD experiments were performed by adding portions of the compound stock solution into the solution of a polynucleotide. In fluorimetric experiments excitation wavelengths of $\lambda_{\text{exc}} = 350, 370$ and 390 nm were used to avoid the inner filter effect caused due by increasing absorbance of the polynucleotide

(Figures S3 and S4). Emission was collected in the range $\lambda_{em} = 400\text{--}600$ nm (SI). Thermal melting curves for DNA, RNA and their complexes with studied compounds were determined as previously described by following the absorption change at 260 nm as a function of temperature. The absorbance of the ligands was subtracted from every curve and the absorbance scale was normalized. T_m values are the midpoints of the transition curves determined from the maximum of the first derivative and checked graphically by the tangent method. Every ΔT_m value here reported was the average of two measurements.

4. Conclusions

Within this manuscript, the design, synthesis, structural characterization and biological activity, including antitumor and antibacterial activity in vitro, of novel 2,5-disubstituted furane derivatives bearing benzimidazole or benzothiazole nuclei has been described. The compounds were prepared by using optimized conventional synthetic methods for benzazole derivatives and were substituted with cyano or amidino group on benzazole nuclei as well as with nitro or chloro substituent on furane ring.

Small molecules that target DNA have attracted significant biochemical and biological scientific interest, either by affecting interactions with proteins involved in replication, gene expression and recombination or as spectrophotometric diagnostic tools [53–55]. In particular, consecutive AT base pairs participate in DNA bending that can have a functional role in the control of cellular processes [56]. In contrast to ctDNA, the presence of the nitro group or chlorine in selected furane-benzothiazole structures did not influence the binding mode with AT-DNA.

All compounds dominantly bound inside the minor groove of AT-DNA either in form of monomer or dimer and higher-order aggregates. Compound **15** could differentiate between alternating and non-alternating shapes of AT-DNA by induced CD signal.

The results obtained from testing by using 2D and 3D cell culture methods on three human lung cancer cell lines A549, HCC827 and NCI-H358 results revealed compounds with high potential antitumor activity (**5**, **6**, **8**, **9** and **15**). In general, benzothiazole derivatives were more active in comparison to benzimidazole derivatives with exception of benzimidazole **15**.

The same compounds showed also high activity against *S. cerevisiae*; therefore, we assume that activity is the consequence of toxicity on eukaryotic cells, which is not an uncommon finding for potential oncology drugs.

However, according to antiproliferative effects, compounds **5**, **6**, **8** and **9** have a high potential to stop the proliferation of cells and in this way provide antitumor activity, which is a common mode of action of many chemotherapeutics. Additionally, some active compounds (**5** and **9**) showed a shift of activity in 3D cytotoxicity and antiproliferative assay from very active to mildly active compounds, which means that in a natural condition such compounds could be less toxic but still effective against tumor growth and therefore they could be promising new antitumor drugs.

Supplementary Materials: The following are available online. Figure S1–S4: spectroscopic characterization of compounds; Figure S5: fluorimetric titrations; Figures S6 and S7: thermal melting experiments; Figure S8: CD experiments; Table S1: electronic absorption data; Table S2: binding constants.

Author Contributions: Synthesis and characterization of targeted compounds: L.R., N.P., M.C. and M.H.; antiproliferative and antibacterial activity in vitro: I.Z., V.R., M.B. and K.B.; interaction with ct-DNA: S.S. and M.R.S.; writing—original draft preparation: L.R., M.R.S., K.B. and M.H. All authors have read and agreed to the published version of the manuscript.

Funding: We greatly appreciate the financial support of the Croatian Science Foundation under projects IP-2018-01-4379 entitled *Exploring the antioxidative potential of benzazole scaffold in the design of novel antitumor agents* and IP-2018-01-4694 entitled *Molecular recognition of DNA:RNA hybrid and multistranded structures in bioanalytical and in vitro systems*.

Institutional Review Board Statement: Not applicable.

Informed Consent Statement: Not applicable.

Conflicts of Interest: The authors declare no conflict of interest. The funders had no role in the design of the study; in the collection, analyses, or interpretation of data; in the writing of the manuscript, or in the decision to publish the results.

Sample Availability: Not available.

References

1. Silverman, R.B. *The Organic Chemistry of Drug Design and Drug Action*; Elsevier Academic Press: Amsterdam, The Netherlands, 2004.
2. Sharma, P.C.; Sinhmar, A.; Sharma, A.; Rajak, H.; Pal Pathak, D. Medicinal significance of benzothiazole scaffold: An insight view. *J. Enzyme Inhib. Med. Chem.* **2013**, *28*, 240–266. [[CrossRef](#)] [[PubMed](#)]
3. Bansal, Y.; Silakari, O. The therapeutic journey of benzimidazoles: A review. *Bioorg. Med. Chem.* **2012**, *20*, 6208–6236. [[CrossRef](#)] [[PubMed](#)]
4. Yadav, G.; Ganguly, S. Structure activity relationship (SAR) study of benzimidazole scaffold for different biological activities: A mini-review. *Eur. J. Med. Chem.* **2015**, *97*, 419–443. [[CrossRef](#)] [[PubMed](#)]
5. Irfan, A.; Batool, F.; Naqvi, S.A.Z.; Islam, A.; Osman, S.M.; Nocentini, A.; Alissa, S.A.; Supuran, C.T. Benzothiazole derivatives as anticancer agents. *J. Enzyme Inhib. Med. Chem.* **2019**, *35*, 265–279. [[CrossRef](#)] [[PubMed](#)]
6. Shah, K.; Chhabra, S.; Shrivastava, S.K.; Mishra, P. Benzimidazole: A promising pharmacophore. *Med. Chem. Res.* **2013**, *22*, 5077–5104. [[CrossRef](#)]
7. Rescifina, A.; Zagni, C.; Varrica, M.G.; Pistarà, V.; Corsaro, A. Recent advances in small organic molecules as DNA intercalating agents: Synthesis, activity, and modeling. *Eur. J. Med. Chem.* **2014**, *74*, 95–115. [[CrossRef](#)] [[PubMed](#)]
8. Rupinder Gill, K.; Rawal, R.K.; Bariwal, J. Recent Advances in the Chemistry and Biology of Benzothiazoles. *Arch. Pharm. Chem. Life Sci.* **2015**, *348*, 155–178. [[CrossRef](#)]
9. Buric, A.J.; Dickerhoff, J.; Yang, D. Novel DNA Bis-Intercalator XR5944 as a Potent Anticancer Drug—Design and Mechanism of Action. *Molecules* **2021**, *26*, 4132. [[CrossRef](#)]
10. Khadieva, A.; Mostovaya, O.; Padnya, P.; Kalinin, V.; Grishaev, D.; Tumakov, D.; Stoikov, I. Arylamine Analogs of Methylene Blue: Substituent Effect on Aggregation Behavior and DNA Binding. *Int. J. Mol. Sci.* **2021**, *22*, 5847. [[CrossRef](#)]
11. Wróbel, A.; Baradyn, M.; Ratkiewicz, A.; Droydowska, D. Synthesis, Biological Activity, and Molecular Dynamics Study of Novel Series of a Trimethoprim Analogs as Multi-Targeted Compounds: Dihydrofolate Reductase (DHFR) Inhibitors and DNA-Binding Agents. *Int. J. Mol. Sci.* **2021**, *22*, 3685. [[CrossRef](#)]
12. Depauw, S.; Lambert, M.; Jambon, S.; Paul, A.; Peixoto, P.; Nhili, R.; Marongiu, L.; Figeac, M.; Dassi, C.; Paul-Constant, C.; et al. Heterocyclic Diamidine DNA Ligands as HOXA9 Transcription Factor Inhibitors: Design, Molecular Evaluation, and Cellular Consequences in a HOXA9-Dependant Leukemia Cell Model. *J. Med. Chem.* **2019**, *62*, 1306–1329. [[CrossRef](#)]
13. Patel, A.; Smith, H.J.; Sturzebecher, J. *Introduction to the Principles of Drug Design and Action*; Smith, H.J., Ed.; CRC Taylor & Francis: Boca Raton, FL, USA, 2006.
14. Tanius, F.A.; Hamelberg, D.; Bailly, C.; Czarny, A.; Boykin, D.W.; Wilson, W.D. DNA Sequence Dependent Monomer–Dimer Binding Modulation of Asymmetric Benzimidazole Derivatives. *J. Am. Chem. Soc.* **2004**, *126*, 143–153. [[CrossRef](#)]
15. Racané, L.; Tralić-Kulenović, V.; Kraljević Pavelić, S.; Ratkaj, I.; Peixoto, P.; Nhili, R.; Depauw, S.; Hildebrand, M.P.; David-Cordonnier, M.H.; Pavelić, K.; et al. Novel Diamidino-Substituted Derivatives of Phenyl Benzothiazolyl and Dibenzothiazolyl Furans and Thiophenes: Synthesis, Antiproliferative and DNA Binding Properties. *J. Med. Chem.* **2010**, *53*, 2418–2432. [[CrossRef](#)]
16. Racané, L.; Kraljević Pavelić, S.; Nhili, R.; Depauw, S.; Paul-Constant, C.; Ratkaj, I.; David-Cordonnier, M.H.; Pavelić, K.; Tralić-Kulenović, V.; Karminski-Zamola, G. New anticancer active and selective phenylene-bisbenzothiazoles: Synthesis, antiproliferative evaluation and DNA binding. *Eur. J. Med. Chem.* **2013**, *63*, 882–891. [[CrossRef](#)] [[PubMed](#)]
17. Hranjec, M.; Kralj, M.; Piantanida, I.; Sedić, M.; Šuman, L.; Pavelić, K.; Karminski-Zamola, G. Novel Cyano- and Amidino-Substituted Derivatives of Styryl-2-Benzimidazoles and Benzimidazo[1,2-*a*]quinolines. Synthesis, Photochemical Synthesis, DNA Binding, and Antitumor Evaluation, Part 3. *J. Med. Chem.* **2007**, *50*, 5696–5711. [[CrossRef](#)]
18. Perin, N.; Nhili, R.; Ester, K.; Laine, W.; Karminski-Zamola, G.; Kralj, M.; David-Cordonnier, M.H.; Hranjec, M. Synthesis, antiproliferative activity and DNA binding properties of novel 5-Aminobenzimidazo[1,2-*a*]quinoline-6-carbonitriles. *Eur. J. Med. Chem.* **2014**, *80*, 218–227. [[CrossRef](#)] [[PubMed](#)]
19. Loncar, B.; Perin, N.; Mioc, M.; Bocek, I.; Grgic, L.; Kralj, M.; Tomic, S.; Radic Stojkovic, M.; Hranjec, M. Novel amino substituted tetracyclic imidazo[4,5-*b*]pyridine derivatives: Design, synthesis, antiproliferative activity and DNA/RNA binding study. *Eur. J. Med. Chem.* **2021**, *217*, 113342. [[CrossRef](#)] [[PubMed](#)]
20. Racané, L.; Stojković, R.; Tralić-Kulenović, V.; Cerić, H.; Đaković, M.; Ester, K.; Mišir Krpan, A.; Radić Stojković, M. Interactions with polynucleotides and antitumor activity of amidino and imidazoliny substituted 2-phenylbenzothiazole mesylates. *Eur. J. Med. Chem.* **2014**, *86*, 406–419. [[CrossRef](#)]
21. Cindrić, M.; Jambon, S.; Harej, A.; Depauw, S.; David-Cordonnier, M.H.; Kraljević Pavelić, S.; Karminski-Zamola, G.; Hranjec, M. Novel amidino substituted benzimidazole and benzothiazole benzo[*b*]thieno-2-carboxamides exert strong antiproliferative and DNA binding properties. *Eur. J. Med. Chem.* **2017**, *136*, 468–479. [[CrossRef](#)]

22. King, H.; Lourie, E.M.; Yorke, W. Studies in chemotherapy. XIX. Further report on new trypanocidal substances. *Ann. Trop. Med. Parasitol.* **1938**, *32*, 177–192. [CrossRef]
23. Lourie, E.M.; Yorke, W. Studies in chemotherapy. XVI. The trypanocidal action of synthalin. *Ann. Trop. Med. Parasitol.* **1939**, *33*, 289–304. [CrossRef]
24. Lombardy, R.L.; Tanius, F.A.; Ramachandran, K.; Tidwell, R.R.; Wilson, W.D. Synthesis and DNA Interactions of Benzimidazole Derivatives Which Have Activity against Opportunistic Infections. *J. Med. Chem.* **1996**, *39*, 1452–1462. [CrossRef] [PubMed]
25. Blagburn, B.L.; Sundermann, C.A.; Lindsay, D.S.; Hall, J.E.; Tidwell, R.R. Inhibition of *Cryptosporidium parvum* in neonatal Hsd:(ICR)BR Swiss mice by polyether ionophores and aromatic amidines. *Antimicrob. Agents Chemother.* **1991**, *35*, 1520–1523. [CrossRef] [PubMed]
26. Mazur, S.; Tanius, F.; Ding, D.; Kumar, A.; Boykin, D.W.; Neidle, S.; Wilson, W.D. A thermodynamic and structural analysis of DNA minor-groove complex formation. *J. Mol. Biol.* **2000**, *300*, 321–337. [CrossRef]
27. Das, B.P.; Boykin, D.W. Synthesis and antiprotozoal activity of 2,5-bis(4-guanylphenyl)thiophenes and -pyrroles. *J. Med. Chem.* **1977**, *20*, 1219–1221. [CrossRef] [PubMed]
28. Tidwell, R.R.; Bell, C.A. *Pentamidine and Related Compounds in Treatment of Pneumocystis Carinii Infection*. *Pneumocystis carinii*; Marcel Dekker: New York, NY, USA, 1993; p. 561.
29. Hopkins, K.T.; Wilson, W.D.; Bender, B.C.; McCurdy, D.R.; Hall, J.E.; Tidwell, R.R.; Kumar, A.; Bajic, M.; Boykin, D.W. Extended aromatic furan amidino derivatives as anti-Pneumocystis carinii agents. *J. Med. Chem.* **1998**, *41*, 3872–3878. [CrossRef] [PubMed]
30. Boykin, D.W.; Kumar, A.; Xiao, G.; Wilson, W.D.; Bender, B.C.; McCurdy, D.R.; Hall, J.E.; Tidwell, R.R. 2,5-Bis[4-(N-alkylamidino)phenyl]furans as Anti-Pneumocystis carinii Agents. *J. Med. Chem.* **1998**, *41*, 124–129. [CrossRef]
31. Ismail, M.A.; Brun, R.; Easterbrook, J.D.; Tanius, F.A.; Wilson, W.D.; Boykin, D.W. Synthesis and Antiprotozoal Activity of Aza-Analogues of Furamidine. *J. Med. Chem.* **2003**, *46*, 4761–4769. [CrossRef] [PubMed]
32. Brajša, K.; Trzun, M.; Zlatar, I.; Jelić, D. Three-dimensional cell cultures as a new tool in drug discovery. *Period. Biliogorum* **2016**, *118*, 59–65. [CrossRef]
33. Zlatar, I.; Jelić, D.; Kelava, V.; Cindrić, M.; Jarak, I.; Koštrun, S.; Karminski-Zamola, G.; Gabelica Marković, V.; Hranjec, M.; Brajša, K. Comparison of Antitumor Activity of Some Benzothiofene and Thienothiofene Carboxanilides and Quinolones in 2D and 3D Cell Culture System. *Croat. Chem. Act.* **2017**, *90*, 413–424. [CrossRef]
34. Perin, N.; Bobanović, K.; Zlatar, I.; Jelić, D.; Kelava, V.; Koštrun, S.; Gabelica Marković, V.; Brajša, K.; Hranjec, M. Antiproliferative activity of amino substituted benzo[b]thieno[2,3-b]pyrido[1,2-a]benzimidazoles explored by 2D and 3D cell culture system. *Eur. J. Med. Chem.* **2017**, *125*, 722–735. [CrossRef] [PubMed]
35. Alotaibi, S.H.; Momen, A.A. Anticancer Drugs' Deoxyribonucleic Acid (DNA) Interactions. In *Biophysical Chemistry-Advance Applications*; Khalid, M., Ed.; IntechOpen: London, UK, 2019; Available online: <https://www.intechopen.com/books/biophysical-chemistry-advance-applications/anticancer-drugs-deoxyribonucleic-acid-dna-interactions> (accessed on 14 July 2021). [CrossRef]
36. Racané, L.; Ptiček, L.; Fajdetic, G.; Tralić-Kulenović, V.; Klobučar, M.; Kraljević Pavelić, S.; Perić, M.; Čipčić Paljetak, H.; Verbanac, D.; Starčević, K. Green synthesis and biological evaluation of 6-substituted-2-(2-hydroxy/methoxy phenyl)benzothiazole derivatives as potential antioxidant, antibacterial and antitumor agents. *Bioorg. Chem.* **2020**, *95*, 103537. [CrossRef] [PubMed]
37. Racané, L.; Tralić-Kulenović, V.; Mihalić, Z.; Pavlović, G.; Karminski-Zamola, G. Synthesis of new amidino-substituted 2-aminothiophenoles: Mild basic ring opening of benzothiazole. *Tetrahedron* **2008**, *64*, 11594–11602. [CrossRef]
38. Hranjec, M.; Pavlović, G.; Marjanović, M.; Karminski-Zamola, G. Benzimidazole derivatives related to 2,3-acrylonitriles, benzimidazo[1,2-a]quinolines and fluorenes. *Eur. J. Med. Chem.* **2010**, *45*, 2405–2417. [CrossRef]
39. Estman, A. Improving anticancer drug development begins with cell culture: Misinformation perpetrated by the misuse of cytotoxicity assays. *Oncotarget* **2017**, *8*, 8854–8866. [CrossRef]
40. Mosmann, T. Rapid colorimetric assay for cellular growth and survival: Application to proliferation and cytotoxicity assays. *J. Immunol. Methods* **1983**, *65*, 55–63. [CrossRef]
41. Parish, J. *Principles of Nucleic Acid Structure*; Saenger, W., Ed.; Springer: New York, NY, USA, 1984; p. 556, DM 79; ISBN 3-540-90761-0.
42. Scatchard, G. The attractions of proteins for small molecules and ions. *Ann. N. Y. Acad. Sci.* **1949**, *51*, 660–672. [CrossRef]
43. Mergny, J.L.; Lacroix, L. Analysis of thermal melting curves. *Oligonucleotides* **2003**, *13*, 515–537. [CrossRef] [PubMed]
44. Demeunynck, M.; Bailly, C.; Wilson, W.D. *DNA and RNA Binders: From Small Molecules to Drugs*; Wiley-VCH: Weinheim, Germany, 2002; Volume 1, Chapter 5.
45. Rodger, A.; Nordén, B. *Circular Dichroism and Linear Dichroism*; Oxford University Press: New York, NY, USA, 1997.
46. Eriksson, M.; Nordén, B. Linear and circular dichroism of drug-nucleic acid complexes. *Methods Enzymol.* **2001**, *340*, 68–98.
47. Šmidlehner, T.; Piantanida, I.; Pescitelli, G. Polarization spectroscopy methods in the determination of interactions of small molecules with nucleic acids—tutorial. *Beilstein J. Org. Chem.* **2017**, *14*, 84–105. [CrossRef] [PubMed]
48. Jezuita, A.; Ejsmont, K.; Szatyłowicz, H. Substituent effects of nitro group in cyclic compounds. *Struct. Chem.* **2021**, *32*, 179–203. [CrossRef]
49. Neidle, S. *Oxford Handbook of Nucleic Acid Structure*; Oxford University Press: Oxford, UK, 1999.
50. Ganushchak, N.I.; Lesyuk, A.I.; Fedorovich, I.S.; Obushak, N.D.; Andrushko, V.N. 5-Aryl-2-furaldehydes in the Synthesis of 2-Substituted 1,3-Benzazoles. *Russ. J. Org. Chem.* **2003**, *39*, 1295–1300. [CrossRef]

51. Chaires, J.B.; Dattagupta, N.; Crothers, D.M. Studies on interaction of anthracycline antibiotics and deoxyribonucleic acid: Equilibrium binding studies on the interaction of daunomycin with deoxyribonucleic acid. *Biochemistry* **1982**, *21*, 3933–3940. [[CrossRef](#)]
52. Chalikian, T.V.; Volker, J.; Plum, G.E.; Breslauer, K.J.A. A more unified picture for the thermodynamics of nucleic acid duplex melting: A characterization by calorimetric and volumetric techniques. *Proc. Natl. Acad. Sci. USA* **1999**, *96*, 7853–7858. [[CrossRef](#)] [[PubMed](#)]
53. Trinquet, E.; Mathis, G. Fluorescence technologies for the investigation of chemical libraries. *Mol. Biosyst.* **2006**, *2*, 380–387. [[CrossRef](#)]
54. Kurutos, A.; Crnolatac, I.; Orehovec, I.; Gadjev, N.; Piantanida, I.; Deligeorgiev, T. Novel synthetic approach to asymmetric monocationic trimethine cyanine dyes derived from N-ethyl quinolinium moiety. Combined fluorescent and ICD probes for AT-DNA labelling. *J. Lumin.* **2016**, *174*, 70–76. [[CrossRef](#)]
55. Tumir, L.M.; Crnolatac, I.; Deligeorgiev, T.; Vasilev, A.; Kaloyanova, S.; Grabar Branilović, M.; Tomić, S.; Piantanida, I. Kinetic Differentiation between Homo- and Alternating AT DNA by Sterically Restricted Phosphonium Dyes. *Chem. Eur. J.* **2012**, *18*, 3859–3864. [[CrossRef](#)]
56. Stefl, R.; Wu, H.; Ravindranathan, S.; Sklenář, V.; Feigon, J. DNA A-tract bending in three dimensions: Solving the dA4T4 vs. dT4A4 conundrum. *Proc. Natl. Acad. Sci. USA* **2004**, *101*, 1177–1182. [[CrossRef](#)] [[PubMed](#)]